50272-101

REPORT DOCUMENTATION PAGE	1. REPORT NO. NSF/RA-780529	2.	PB 292798

4. Title and Subtitle

Simple Models for Computing Dynamic Responses of Complex Frame Structures

April 1978

6.

7. Author(s)

C.C. Chen, C.T. Sun, J.L. Bogdanoff, H. Lo

8. Performing Organization Rept. No.

9. Performing Organization Name and Address

Purdue University
School of Aeronautics and Astronautics
West Lafayette, Indiana 47907

10. Project/Task/Work Unit No.

11. Contract(C) or Grant(G) No.

(C)

(G) GI41897

12. Sponsoring Organization Name and Address

Applied Science and Research Applications (ASRA)
National Science Foundation
1800 G Street, N.W.
Washington, D.C. 20550

13. Type of Report & Period Covered

14.

15. Supplementary Notes

16. Abstract (Limit: 200 words)

Prohibitive costs of analyzing large frame structures using the finite element method have led researchers to investigate simpler procedures of analysis. The development of a simple shear beam and a Timoshenko base model for dynamic analysis of complex frame structures is described. Formulas are derived for computing the equivalent shear and bending rigidities of the structure. Simple models are evaluated by comparing simple model solutions with solutions obtained from using full scale finite elements in free vibrations of plane frames. It was found that the simple models yield very accurate frequencies as well as mode shapes for the lower modes, and the Timoshenko model is more superior to the shear beam model when diagonal bracings are present. When the shear beam model was employed to compute the natural frequencies of a TVA fossil fuel power plant at Paradise, Kentucky, the first two frequencies were found to be in good agreement with the finite element solutions. The simple models were also used to compute transient dynamic responses of structures subjected to earthquake disturbances. Evaluative examples and dynamic internal force and moment computations using simple models are included.

17. Document Analysis a. Descriptors

Framed structures
Models
Shear properties
Earthquakes
Analyzing
Kentucky
Electric power plants
Frequency measurement
Earthquake resistant structures
Dynamic structural analysis

b. Identifiers/Open-Ended Terms

Finite element method
Shear beam model
Timoshenko base model

c. COSATI Field/Group

18. Availability Statement	19. Security Class (This Report)	21
NTIS	20. Security Class (This Page)	22. Price PC A05/MF A01

Acknowledgement

The support of the National Science Foundation under Grant No. GI-41897 is gratefully acknowledged.

Abstract

A simple shear beam and a Timoshenko beam model have been developed for dynamic analysis of complex frame structures. Explicit formulas have been derived for computing the equivalent shear and bending rigidities of the structure. The simple models were evaluated by comparing the simple model solutions with the solutions obtained from using full scale finite elements in free vibrations of plane frames. It was found that the simple models yielded very accurate frequencies as well as mode shapes for the lower modes. When diagonal bracings are present, the Timoshenko beam model was more superior to the shear beam model. The shear beam model was employed to compute the natural frequencies of the fossil fuel power plant of Unit #3 of TVA at Paradise, Kentucky. The first two frequencies were found to be in good agreement with the finite element solutions. The simple models were also used to compute transient dynamic responses of structures subjected to earthquake disturbances.

Table of Contents

1. Introduction

Dynamic analyses of large frame structures such as the structures in a fossil fuel power plant can be performed by using the finite element method. However, such analyses are usually very laborious and require a great amount of computer time. In many cases, this type of analysis can prove to be prohibitive. Simple procedures of analysis are obviously desirable.

Several approximate analyses for vibration of plane frame structures have been employed in recent years. The fundamental slope-deflection formulas were used by Goldberg, Bogdanoff, and Moh [1] to set up two classes of equilibrium equations, i.e., shear equations and joint equations, for each story. The method they developed was a trial-and-error technique for determining the natural frequencies, mode shapes, and the response to ground motion. A modifed and extended iterative method was presented by Paramasivam, Yeh, and Nassim [2] who took into account different individual joint rotations. The successive approximation scheme used by [1] and [2] is a tedious process. The other main drawback is that the effect of bracing cannot be included. Sandhu [3] has presented a simplified method based upon the concept of an elastic shear wave equation in a uniform solid bar to model the dynamic behavior of multi-story plane frame structures. The results based upon the model given in [3] were not accurate even for a homogeneous four-bay, six-story structure chosen for illustration. Heidebrecht and Smith [4] have suggested a shear-flexural beam model to perform dynamic analysis for tall wall-frame structures. The concept for evaluating the shear rigidity may be adopted for investigating simple shear beam model for vibration of plane frames. An interesting method was presented by Blume [5,6] who developed

simple procedures with which the contribution of story shear, joint rotation, overall flexural, and ground compliance in the three lowest modes of vibration could be estimated. A period synthesis concept and the pseudo-stiffness procedures were presented to enable the approximate determination of natural periods as well as mode shapes for rigid-floor shear buildings. However, it is required to provide charts for certain case studies before the method can be employed.

This research concerns developing simple models for computing dynamic responses of complex frame structures. A shear beam model which is able to account for the girder flexibility is first presented. As long as a structure deflects in shear-type, fairly accurate results can be expected. When the gross flexural deformation becomes significant, the Timoshenko beam model is then used. Explicit formulas for shear and bending rigidities of the models are derived in terms of the member dimensions and material properties of the original frame structure. Several plane frame structures are first used as evaluative examples. Free vibrations of these structures are investigated by finite element method as well as by using the simple models. Both frequencies and mode shapes predicted by the simple models are in good agreement with those obtained from finite element method. The shear beam model is then used to model the boiler-frame structure of the fossil fuel power plant of TVA Unit #3 at Paradise, Kentucky.

The mode-superposition method is then used for analysis of transient dynamic responses of the simple models. A specific 4-bay and 7-story frame structure subjected to the N-S component of the El Centro 1940 earthquake ground acceleration is studied by both the simple models and the finite element method. The simple models are excellent in the comparison.

A procedure is also developed to recover the dynamic member forces and moments in the actual structure from the representative simple models.

Results obtained by using this procedure are found to be rather accurate.

2. The Simple Models

The use of simple models to represent a frame structure requires determination of the effective shear rigidity GA and effective bending rigidity EI of the frame. Once these properties are established, the vibration analysis is performed in the usual manner. Evaluation of the overall shear and bending rigidities of a frame structure by considering all the members exactly can be done on the computer with the aid of the finite element method. However, such approach apparently defeats the purpose of a simple model. In view of this, the frame structure is first decomposed into several typical substructures and then the contribution of each substructure in the gross shear and bending rigidities is evaluated.

3. Evaluation of the Shear Rigidity

The typical substructures are indicated in Fig. 1. Since the base of the structure is assumed fixed, the behavior of the structural members at the ground level is substantially different from the rest, and, hence, are considered separately. For a tall building where the boundary effect is relatively small, it might not be necessary to make such distinction.

In a lower mode vibration, it is assumed that, away from the base, the deformation is somewhat "smooth" in the longitudinal direction, and consequently the middle point of a column between two adjacent floors could be a point of inflection. Similar argument leads to the conclusion that the midpoint of a girder is a point of inflection. For the present purpose, these points are then replaced by equivalent hings and rollers as shown in Fig. 1. The substructures at the ground level for the shear rigidity analysis are depicted also in Fig. 1.

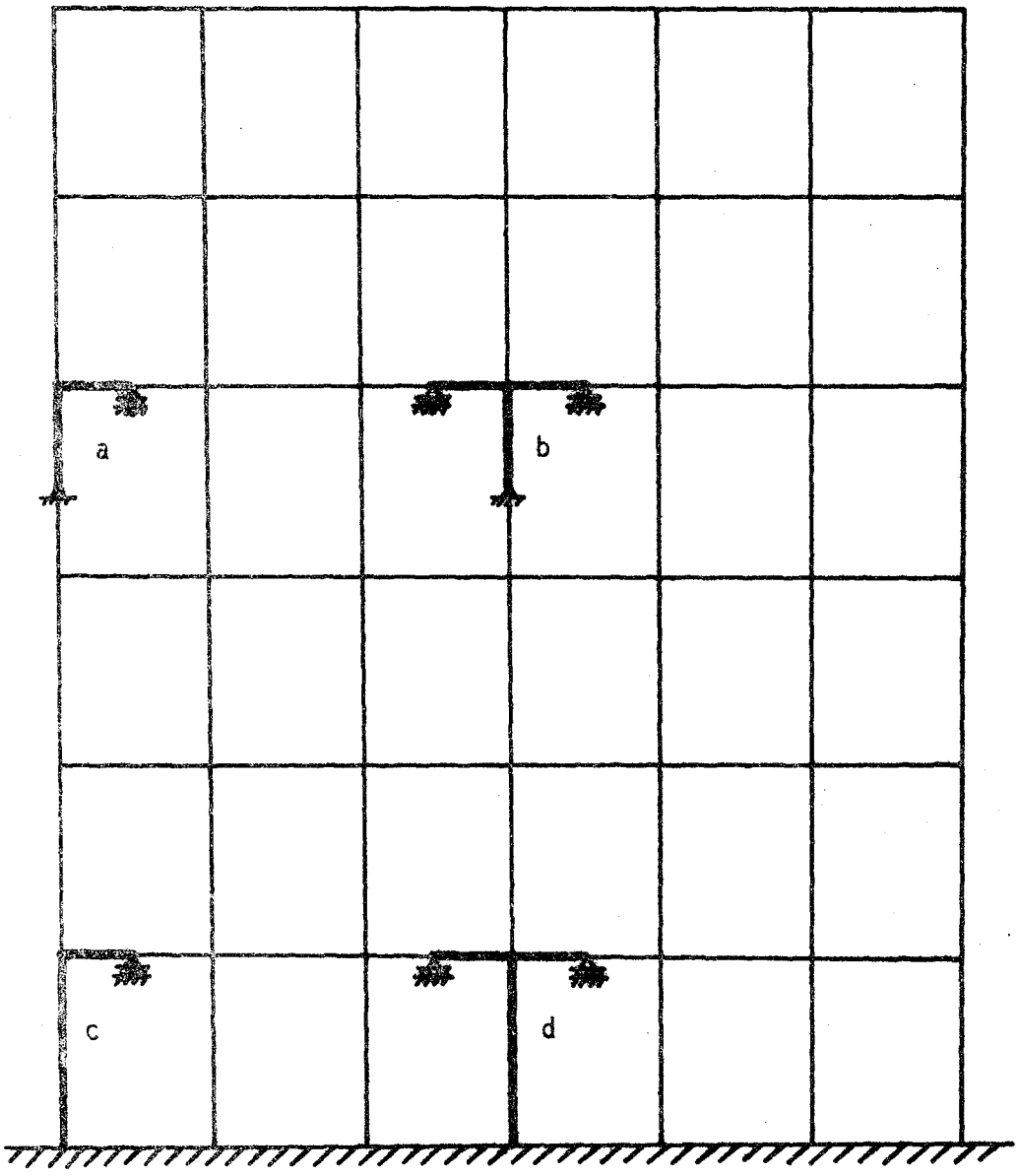

Figure 1 Four types of substructures

To illustrate the procedure for evaluating the effective shear rigidity contributed by the substructures, substructure Type a is first considered. By applying a horizontal force P at the joint as shown in Fig. 2, the corresponding displacement δ can easily be obtained. In this analysis, the rigid frame assumption is taken. In other words, the axial deformation is neglected. The resulting displacement is obtained as

$$\delta = \frac{(2+\alpha\beta)L_c^3}{24\alpha\beta EI_c} P \tag{1}$$

where E is the Young's modulus assumed to be identical for columns and girders, I_c is the moment of inertia of the column, L_c is the column length between two adjacent floors, and α and β are defined by

$$\alpha = I_g/I_c$$
$$\beta = L_c/L_g \tag{2}$$

in which a subscript g denotes girder.

The equivalent shear strain is

$$\gamma = \frac{\delta}{L_c/2} \tag{3}$$

The shear force associated with this amount of shear strain in an equivalent shear beam is

$$(GA)_a\gamma = (GA)_a \frac{2\delta}{L_c} \tag{4}$$

where $(GA)_a$ is the effective shear rigidity provided by the column under consideration. Substitution of Eq. (1) into Eq. (4) yields

$$(GA)_a = \frac{12\alpha\beta EI_c}{(2+\alpha\beta)L_c^2} \tag{5}$$

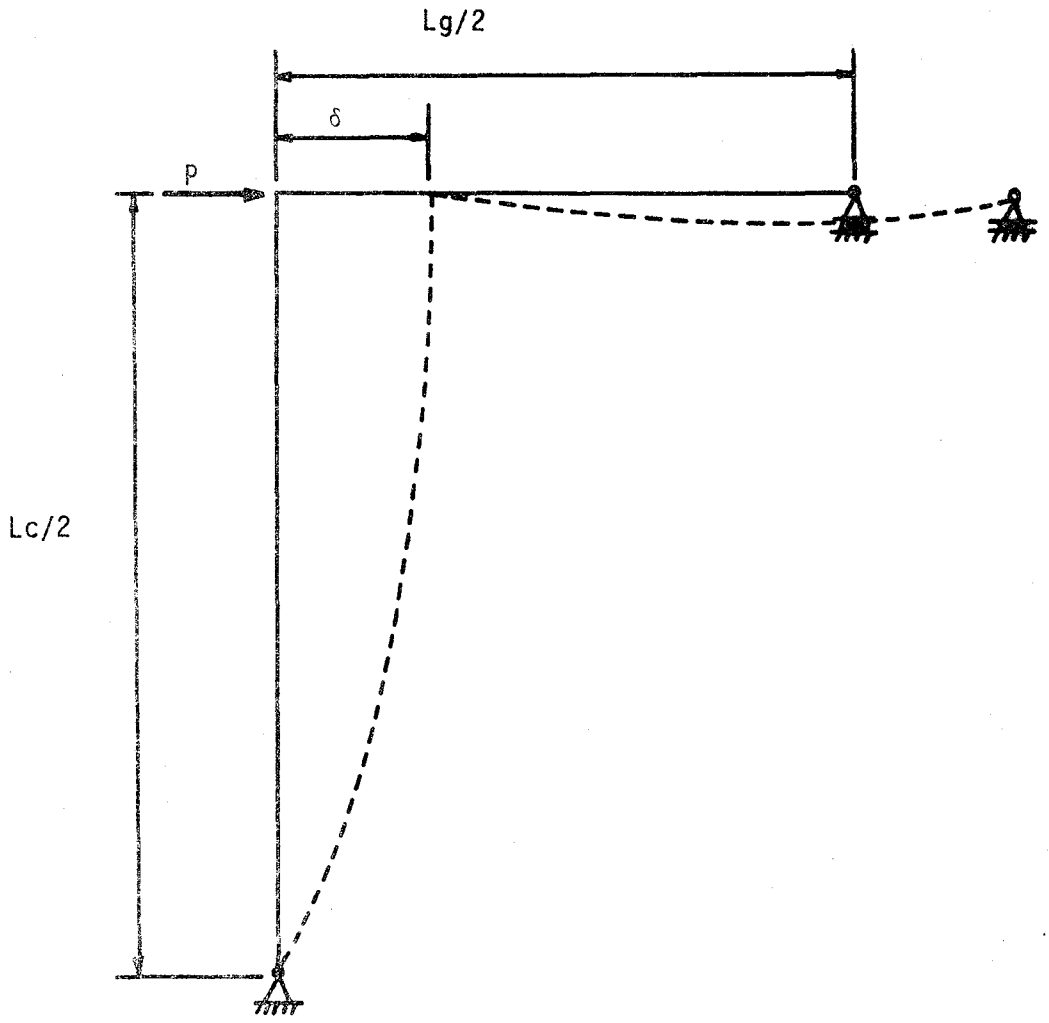

Figure 2 Effective shear rigidity of substructure Type a

for substructure Type a.

Similar procedures lead to the following results for other types of substructures:

$$(GA)_b = \frac{12\alpha\beta EI_c}{(1+\alpha\beta)L_c^2} \tag{6}$$

for substructure Type b,

$$(GA)_c = \frac{12(1+3\alpha\beta)EI_c}{(4+3\alpha\beta)L_c^2} \tag{7}$$

for substructure Type c, and

$$(GA)_d = \frac{6(1+6\alpha\beta)EI_c}{(2+3\alpha\beta)L_c^2} \tag{8}$$

for substructure Type d. The total effective shear rigidity of the frame substructure between two floors is the sum of the shear rigidities of the appropriate substructures.

4. Diagonal Bracings

Diagonal bracing is often used in flexible frames to provide additional lateral resistance against earthquake motion. Since a brace is usually designed to take axial forces only, it can be considered as an axial member without bending rigidity. The additional shear rigidity of the structure due to a brace will be calculated based upon this assumption. It is thus assumed that the braces and frames are pin-connected to each other, so that the bracing stiffness can be added to the frame stiffness. This approach was taken also by Clough and Jenschke in a study on the effect of diagonal bracing on the earthquake performance of a steel frame building [7].

With the foregoing assumptions, the shear rigidity of a brace can be obtained by analyzing the simple problem in Fig. 3a. The additional effective shear rigidity is obtained as

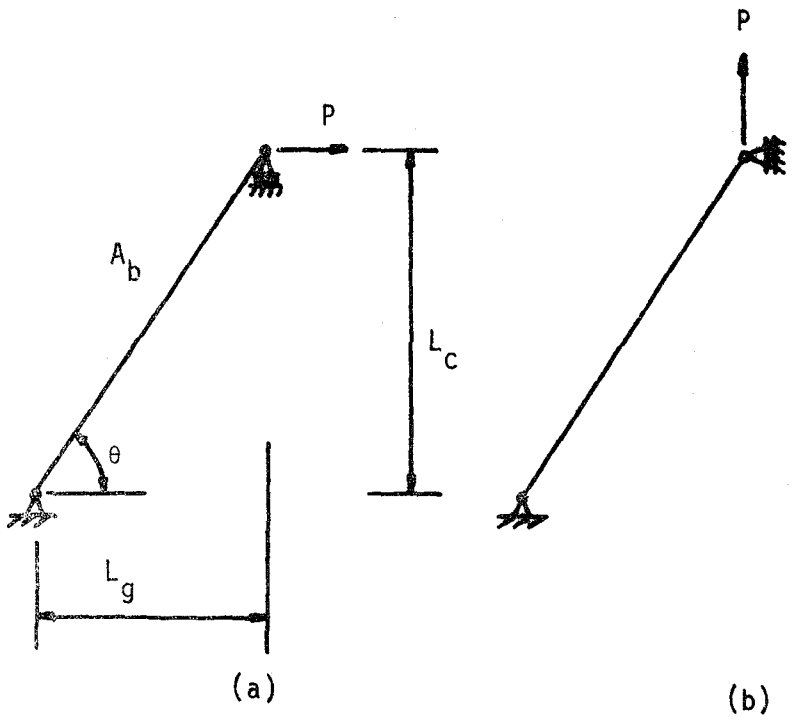

Figure 3 Effective shear and bending rigidities of a brace

$$(GA)_{Br} = A_b E \cos^2 \theta \sin \theta \tag{9}$$

where A_b is the cross-sectional area of the brace and θ is the inclined angle of the brace considered. The above expression can also be re-written as

$$(GA)_{Br} = \frac{\beta}{(1+\beta^2)^{3/2}} A_b E \tag{10}$$

in which β is defined by Eq. (2).

5. Shear Beam Model

In practical applications, a great number of frame structures behave essentially as shear components for the lower mode vibrations. The shear beam model is then considered to be infinitely rigid in bending.

Consider a shear beam finite element of length L, shear rigidity GA, and mass per unit length m. The strain energy and kinetic energy per unit length of beam are given by

$$U_s = \tfrac{1}{2} GA \left(\frac{\partial v}{\partial x}\right)^2 \tag{11}$$

and

$$T_s = \tfrac{1}{2} m(\dot{v})^2 \tag{12}$$

respectively. In equations (11) and (12), v is the transverse displacement.

In the absence of lateral loadings, the equation of motion can be obtained by using the Hamilton's principle. The resulting equation of motion is expressed as

$$\frac{\partial}{\partial x}\left[GA \frac{\partial v}{\partial x} \right] = m\ddot{v} \tag{13}$$

It is important to note that the present shear beam model is different from the conventional shear beam model for which the floors are assumed to be infinitely stiff as compared to the columns. Besides being able to account for the girder flexibility, the present shear beam model is also more elaborate in evaluating the effective shear rigidity as has been described previously.

To retain the simplicity, the following displacement function is assumed for the shear beam finite element:

$$v = (1 - \frac{x}{L})\, v_1 + \frac{x}{L}\, v_2 \tag{14}$$

where v_1 and v_2 are the nodal displacement and L is the element length. The stiffness matrix then reads

$$[K] = \frac{GA}{L} \begin{bmatrix} 1 & -1 \\ -1 & 1 \end{bmatrix} \tag{15}$$

A lump-mass matrix of the form

$$[M] = \frac{mL}{2} \begin{bmatrix} 1 & 0 \\ 0 & 1 \end{bmatrix} \tag{16}$$

will be used. The lump-mass method, in general, overestimates the inertia effect, and is thus more suitable for the shear beam as the suppression of bending also has a stiffening effect on the structure.

6. The Timoshenko Beam Theory

For convenience of reference, the basic formulation of the Timoshenko beam theory is reviewed first. Consider a Timoshenko beam finite element of length L, bending rigidity EI, shear rigidity GA, mass per unit length m, and rotatory inertia ρI (ρ is the mass density and the moment of inertia I is obtained from the value of EI). Referring to Fig. 4 which shows the

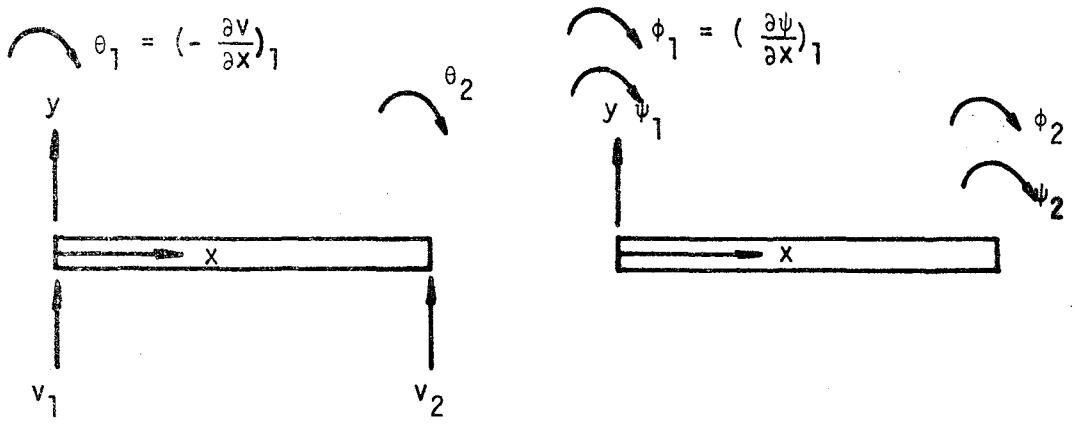

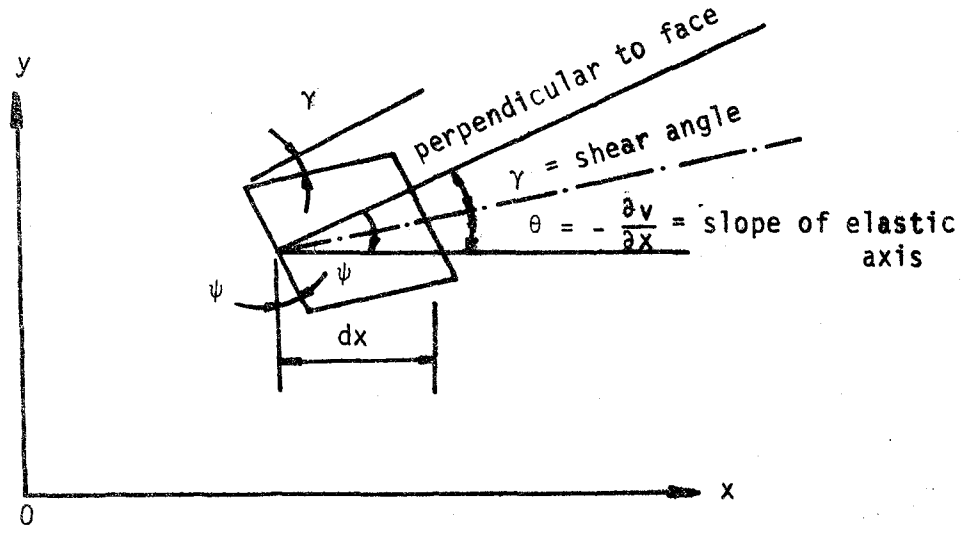

Figure 4 Timoshenko beam element: (a) degrees of freedom; (b) deformation of differential element

coordinate system and degrees of freedom chosen, the strain energy and kinetic energy per unit length of beam are given as follows:

$$U = \tfrac{1}{2}EI\left(\frac{\partial\psi}{\partial x}\right)^2 + \tfrac{1}{2}\kappa GA\left(\frac{\partial v}{\partial x} + \psi\right)^2 \tag{17}$$

and

$$T = \tfrac{1}{2}\, m\,(\dot{v})^2 + \tfrac{1}{2}\,\rho I\,(\dot{\psi})^2 \tag{18}$$

respectively [8]. In addition to the notations denoted previously, ψ represents the bending slope of the cross section of the element.

In the absence of lateral loadings, the equations of motion can also be easily obtained. These two resulting coupled partial differential equations are expressed as

$$\begin{aligned} &\frac{\partial}{\partial x}\left(EI\,\frac{\partial\psi}{\partial x}\right) + \kappa GA\left(\frac{\partial v}{\partial x} + \psi\right) = \rho I\ddot{\psi} \\ &\frac{\partial}{\partial x}\left[\kappa GA\left(\frac{\partial v}{\partial x} + \psi\right)\right] = m\ddot{v} \end{aligned} \tag{19}$$

The shear force Q and the bending moment M are related to the displacements as

$$Q = \kappa GA\left(\frac{\partial v}{\partial x} + \psi\right) \tag{20}$$

and

$$M = EI\,\frac{\partial\psi}{\partial x} \tag{21}$$

respectively. The shear correction coefficient κ assumes different values depending on the geometry of the cross-section. In this study, we set κ = 1.

7. Evaluation of the Bending Rigidity

The gross bending effect can be large for tall building structures. In

the present consideration, it is assumed that the joints of the same floor level displace linearly in the vertical direction with respect to the centroidal axis of the cross-sectional areas of columns as shown in Fig. 5. This assumption is obviously valid only in lower modes of vibration. In addition, it is also assumed that the restoring forces in the vertical direction are provided by the axial forces in columns. Denoting the incremental rotation at a floor level relative to the lower one by ε (see Fig. 5), the relative displasement at joint i is given by

$$\delta_i = d_i \varepsilon \tag{22}$$

where d_i is the horizontal distance from the joint to the centroidal axis. Suppose furthermore that the strain is constant in the column, the corresponding axial force becomes

$$P_i = E(A_c)_i \frac{\delta i}{L_c} = E(A_c)_i \, d_i \, \frac{\varepsilon}{L_c} \tag{23}$$

where $(A_c)_i$ is the cross-sectional area of the i^{th} column. The moment about the centroid due to P_i is

$$M_i = P_i d_i = E(A_c)_i \, d_i^2 \, \varepsilon / L_c \tag{24}$$

The total bending moment of the whole structure is obtained as

$$M = \sum_i M_i = E \frac{\varepsilon}{L_c} \sum_i (A_c)_i \, d_i^2 \tag{25}$$

Equating Eq. (25) to Eq. (21), an equality equation is then followed:

$$EI \frac{\partial \psi}{\partial x} = E \frac{\varepsilon}{L_c} \sum_i (A_c)_i \, d_i^2 \tag{26}$$

where EI represents the effective bending rigidity of the equivalent Timoshenko beam model. Since the strain is assumed constant in columns, it

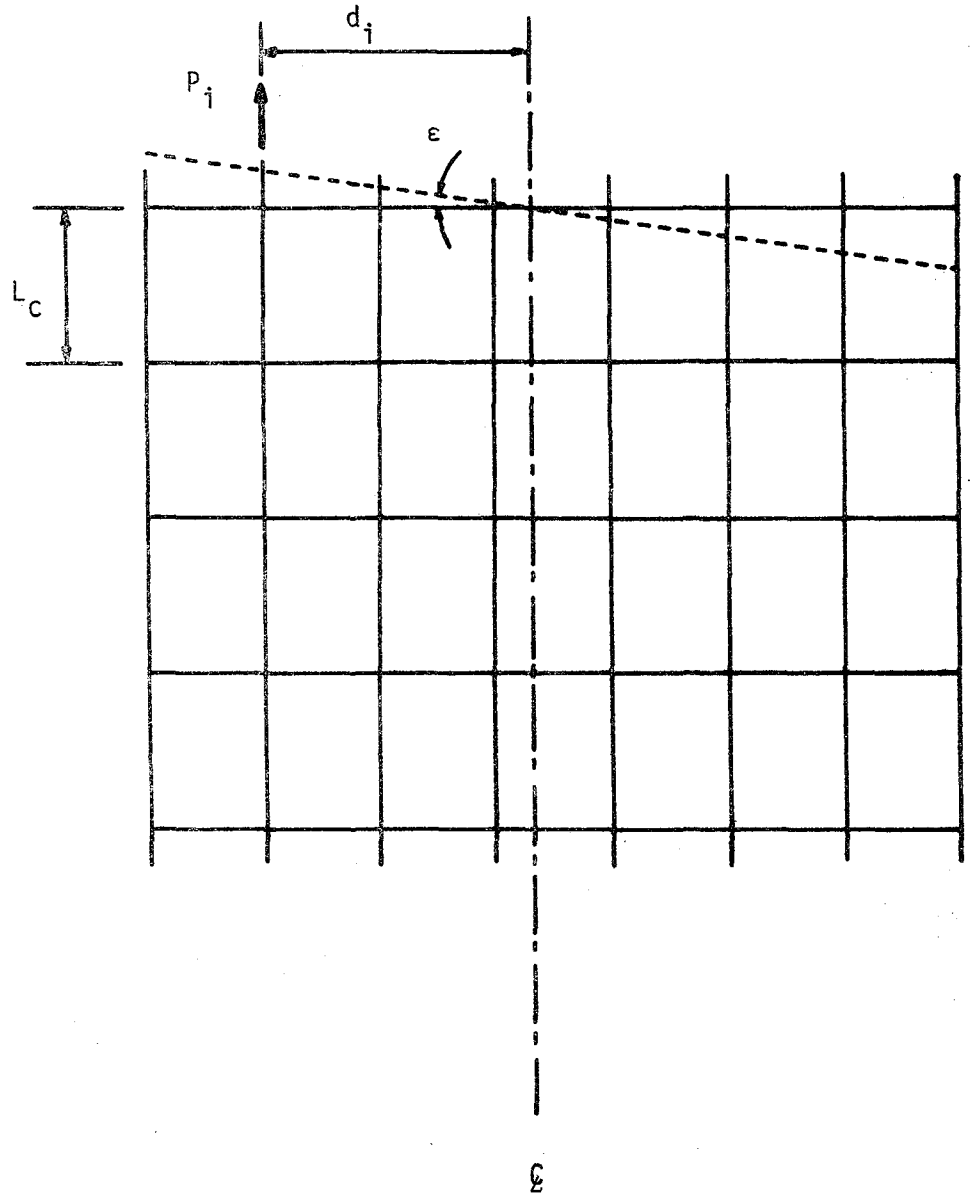

Figure 5 Gross bending deformation

follows that

$$\frac{\partial \psi}{\partial x} = \frac{\varepsilon}{L_c} \tag{27}$$

between any two adjacent floors. As a result, the effective bending rigidity can be expressed in the form

$$EI = E \sum_i (A_c)_i \, d_i^2 \tag{28}$$

Referring to Fig. 3b, the additional effective gross bending rigidity due to a brace can easily be obtained as

$$(EI)_{Br} = EA_b d^2 \sin^3 \theta \tag{29}$$

or

$$(EI)_{Br} = \frac{\beta^3}{(1+\beta^2)^{3/2}} A_b E d^2 \tag{30}$$

in which d denotes the distance between the upper joint of the brace to the centroidal axis of the cross-sectional areas of columns.

8. The Timoshenko Beam Model

Since the resulting equivalent Timoshenko beam for the frame structure is, in general, nonhomogeneous, it will be more convenient to employ the finite element method for solution. Derivation of the stiffness and consistent mass matrices is quite straightforward. Hence, only the results will be presented here.

Consider a Timoshenko beam finite element as described in Sec. 6. By assuming the shape functions for the displacement variables as

$$\begin{aligned} v &= a_0 + a_1 x + a_2 x^2 + a_3 x^3 \\ \psi &= b_0 + b_1 x + b_2 x^2 + b_3 x^3 \end{aligned} \tag{31}$$

together with the energy functions given by Eqs. (17) and (18), the total strain energy and kinetic energy in a Timoshenko beam finite element can be computed. The matrix equations of motion for the discrete system using Hamilton's principle become

$$\{F\} = [K]\{\Delta\} + [M]\{\ddot{\Delta}\} \tag{32}$$

where [K] and [M] are the element stiffness matrix and element mass matrix of order 8 x 8, respectively. In Eq. (32), the force vector {F} and the displacement vector {Δ} of order 8 x 1 are defined by

$$\{F\} = \begin{Bmatrix} Q_1 \\ N_1 \\ M_1 \\ \mu_1 \\ Q_2 \\ N_2 \\ M_2 \\ \mu_2 \end{Bmatrix} \quad \text{and} \quad \{\Delta\} = \begin{Bmatrix} v_1 \\ \theta_1 \\ \psi_1 \\ \psi'_1 \\ v_2 \\ \theta_2 \\ \psi_2 \\ \psi'_2 \end{Bmatrix} \tag{33}$$

respectively. The subscripts 1 and 2 denote node 1 and node 2, respectively, and a prime indicates the slope. It should be noted that with this higher order element, only Q and M can be realized in the boundary conditions; the generalized forces N and μ are set equal to zero at both clamped end and free end. In view of the displacement fields, the boundary conditions are $v = 0$ and $\psi = 0$ at the clamped end and that the bending moment is zero, that is, $\psi' = 0$, and the shear force is zero, that is, $\theta - \psi = 0$, at the free end.

The stiffness matrix is obtained as

$$[K] = \left[\begin{array}{c|c} k_1 & k_2 \\ \hline k_2^T & k_4 \end{array}\right] \tag{34}$$

where the superscript T denotes transpose of the matrix and the submatrices are given by

$$[k_1] = \begin{bmatrix} 504b & -42Lb & -210Lb & -42L^2b \\ & 54L^2b & -42L^2b & 0 \\ & & 36a+156L^2b & 3La+22L^3b \\ \text{Sym.} & & & 4L^2a+4L^4b \end{bmatrix} \tag{35}$$

$$[k_2] = \begin{bmatrix} -504b & -42Lb & -210Lb & 42L^2b \\ 42Lb & -14L^2b & 42L^2b & -7L^3b \\ 210Lb & 42L^2b & -36a+54L^2b & 3La-13L^3b \\ 42L^2b & 7L^3b & -3La+13L^3b & -L^2a-3L^4b \end{bmatrix} \tag{36}$$

and

$$[k_4] = \begin{bmatrix} 504b & 42Lb & 210Lb & -42L^2b \\ & 56L^2b & -42L^2b & 0 \\ & & 36a+156L^2b & -3La-22L^3b \\ \text{Sym.} & & & 4L^2a+4L^4b \end{bmatrix} \tag{37}$$

In Eqs. (35-37),

$$a = \frac{EI}{30L} \quad , \quad b = \frac{\kappa GA}{420L} \tag{38}$$

The mass matrix is expressed in the form

$$[M] = \left[\begin{array}{c|c} m_1 & m_2 \\ \hline m_2^T & m_4 \end{array}\right] \tag{39}$$

where the submatrices are given by

$$[m_1] = \begin{bmatrix} 156c & -22Lc & 0 & 0 \\ & 4L^2c & 0 & 0 \\ & & 156e & 22Le \\ \text{Sym.} & & & 4L^2e \end{bmatrix} \tag{40}$$

$$[m_2] = \begin{bmatrix} 54c & 13Lc & 0 & 0 \\ -13Lc & -3L^2c & 0 & 0 \\ 0 & 0 & 54e & -13Le \\ 0 & 0 & 13Le & -3L^2e \end{bmatrix} \tag{41}$$

and

$$[m_4] = \begin{bmatrix} 156c & 22Lc & 0 & 0 \\ & 4L^2c & 0 & 0 \\ & & 156e & -22Le \\ \text{Sym.} & & & 4L^2e \end{bmatrix} \tag{42}$$

The two parameters c and e in Eqs. (40-42) are

$$c = \frac{\rho AL}{420} \quad , \quad e = \frac{\rho IL}{420} \tag{43}$$

In this study, the consistent mass system is adopted for the Timoshenko beam finite element. It is noted that lumped mass system can also yield acceptable results. The Timoshenko beam model presented herein can also be reduced to the shear beam model by suppressing the rotation ψ in the Timoshenko beam finite element. The same purpose can also be achieved by letting the bending rigidity EI approach infinity.

9. Modifications of Shear Rigidity for Local Bending Effects

The effective shear rigidities presented in Sec. 3 for frame structures and in Sec. 4 for bracings become invalid as the frame structure vibrates

with significant local bending effects. In this case, the shear beam model and Timoshenko beam model developed previously can not yield good solutions. Modifications of the effective shear rigidities for both the framework and bracings at the locations where the local bending effects occur are required. It is noted that the local bending effects are mainly due to the existence of bracings. This fact will become apparent when the evaluative examples #5 and #6 in Sec. 11 are carried out and compared.

To modify the effective shear rigidities, two cases that cause significant local bending are considered, namely, the rotation of the panel of a framework and the stretching of columns and bracings. In the following, these cases are considered separately and a modified gross shear rigidity is evaluated.

Fig. 6a shows a typical panel ABCD and its deformed shape A'B'C'D'. The force P* associated with the shear strain γ is equal to the shear rigidity (GA)* times γ. The force P* is also the difference between the force P associated with the shear strain γ and the force P' associated with the shear strain ξ. Therefore, the effective shear rigidity that accounts for the rotation of pannel can be expressed as

$$(GA)^* = \frac{P^*}{\gamma} = \frac{P-P'}{\gamma} = \frac{(GA)\gamma - (GA)\xi}{\gamma}$$

$$= (1 - \frac{\xi}{\gamma})\ GA \qquad (44)$$

where GA is the shear rigidity evaluated according to the previously unmodified procedure in Sections 3 and 4. Note that the modified shear rigidity (GA)* reduces to the unmodified shear rigidity GA if no panel rotation occurs and that no shear rigidity is provided by the panel as the two shear strains ξ and γ equal. Equation (44) should be used to modify

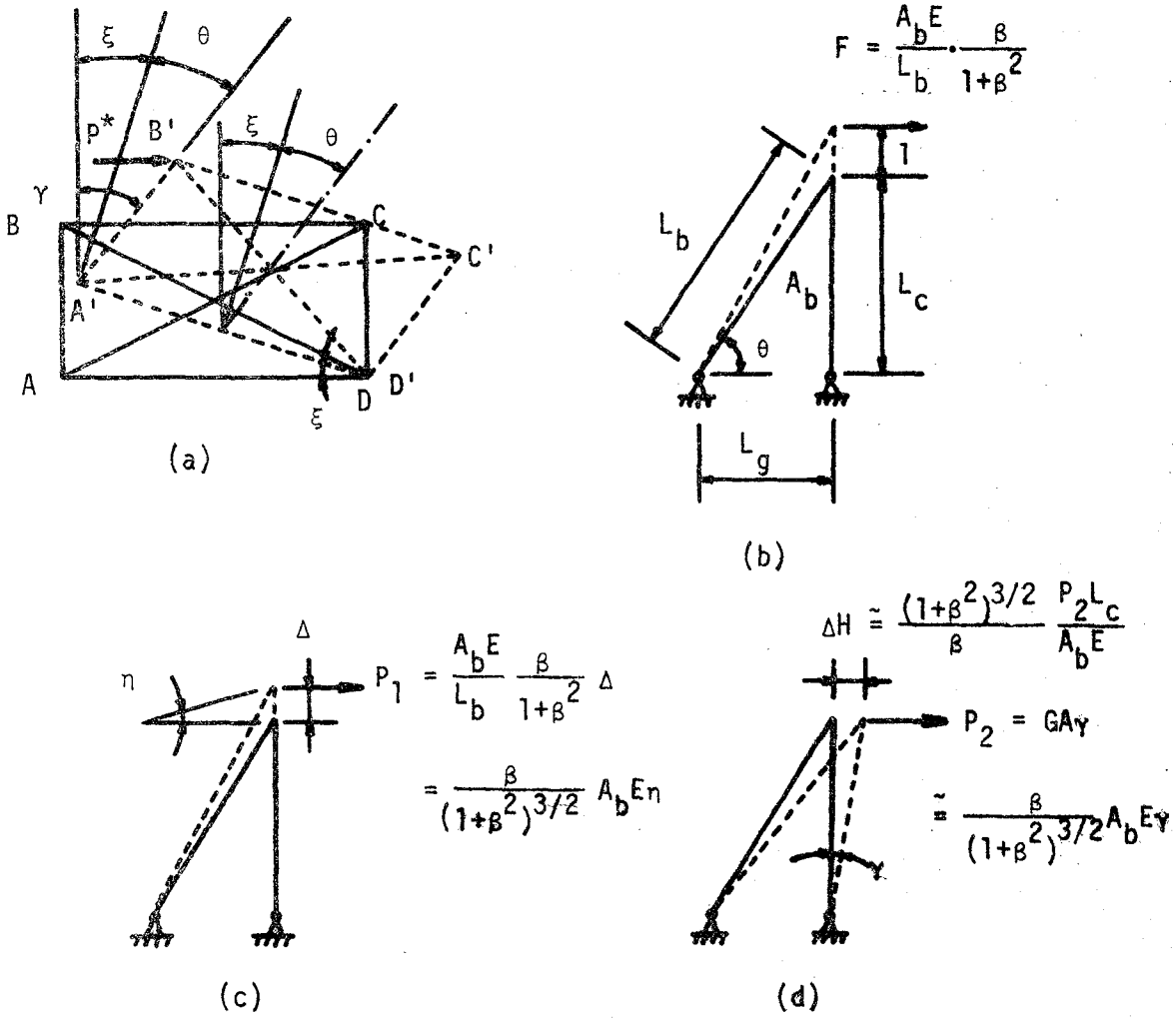

Figure 6 Modification of effective shear rigidity: (a) rotation of panel; (b,c, and d) stretching of panel

the shear rigidities of the substructures involved.

In Sec. 4, the bracing's contribution to the shear rigidity came from the side-sway of the column. When bending is pronounced, columns are stretched so are the bracings. In the following, the additional shear rigidity due to the stretching of columns and bracings is estimated.

Referring to Fig. 6b, the force induced horizontally to raise one unit of vertical displacement is equal to

$$F = \frac{A_b E}{L_b} \sin\theta \cos\theta \tag{45}$$

or

$$F = \frac{A_b E}{L_b} \frac{\beta}{1+\beta^2} \tag{46}$$

in which A_b and L_b are the cross-sectional area and length of the brace considered, respectively. The horizontal force for a Δ-displacement (see Fig. 6c) is expressed in terms of the angle η as

$$P_1 = \frac{A_b E}{L_b} \frac{\beta}{1+\beta^2} \cdot \frac{\Delta}{1} = \frac{A_b E}{L_b} \frac{\beta}{1+\beta^2} \eta L_g$$

$$= \frac{\beta}{(1+\beta^2)^{3/2}} A_b E \eta = (GA)_{Br} \eta \tag{47}$$

where $(GA)_{Br}$ is the effective shear rigidity of a brace given by Eq. (10). The force P_1 is the additional horizontal restoring force due to the vertical deformation. In the shear beam model, the only deformation allowed is the shear strain γ. Thus, an equivalent shear force P_2 should be assigned to represent P_1. Hence,

$$P_2 = (GA)'_{Br} \gamma = P_1 \tag{48}$$

Substitution of Eq. (47) into Eq. (48) yields

$$(GA)'_{Br} = \frac{P_1}{\gamma} = \frac{\eta}{\gamma}(GA)_{Br} \tag{49}$$

Adding Eq. (49) to Eq. (44), we obtain the modified shear rigidity contributed for the bracing as

$$(GA)_{Br} = (1 - \frac{\xi}{\gamma} + \frac{\eta}{\gamma})(GA)_{Br} \tag{50}$$

The above shear rigidity for the brace is needed in the case where local bending effect can not be neglected.

10. Applications to the Three-Dimensional Frame Structures

Many three-dimensional frame structures, in practice, can be regarded as a collection of plane frames connected by girders. Consequently, vibrations in the principal planes can be analyzed by using the shear beam model or the Timoshenko beam model. To derive the representative beam models, we first model the individual plane frames by the beam models and then combine the stiffnesses and masses of these beam models into a single beam model. In such process, relative motions among the individual plane frames are lost, and the gross torsional mode of vibration can not be accounted for. The analysis procedure presented here, however, should be valid for designs where motions in the principal planes are the main concern. In particular, this simple model analysis should be useful in the preliminary design stage.

11 Evaluative Examples

Free vibrations of several plane frame structures of different characteristics are now investigated by the simple models. The complex three-dimensional frame structure of the fossil fuel steam generating plant of Unit #3 of TVA at Paradise, Kentucky is also studied. The simple model solutions are then compared with the conventional finite element solutions using the existing well-developed SAP IV program [9]. The latter solutions are regarded as the exact solutions for comparison purposes.

Example 1: 10 Bay - 9 Story Plane Frame

This first example is purposely taken from one of the sample problems in SAP IV [9] for comparison. The geometry and material constants of the plane frame are given in Fig. 7. The corresponding shear beam model or Timoshenko beam model is also shown. Nine shear beam or Timoshenko beam finite elements are used with the floor mass lumped at the nodes. The mass per unit length, m, of both models is calculated according to

$$m = \sum \rho A_c \tag{51}$$

The effective shear rigidities of the four types of substructures are obtained from Eqs. (5-8) as

$$\begin{aligned}
(GA)_a &= 2.4 \frac{EI_c}{L_c^2} \\
(GA)_b &= 4 \frac{EI_c}{L_c^2} \\
(GA)_c &= \frac{60}{11} \frac{EI_c}{L_c^2} \\
(GA)_d &= \frac{48}{7} \frac{EI_c}{L_c^2}
\end{aligned} \tag{52}$$

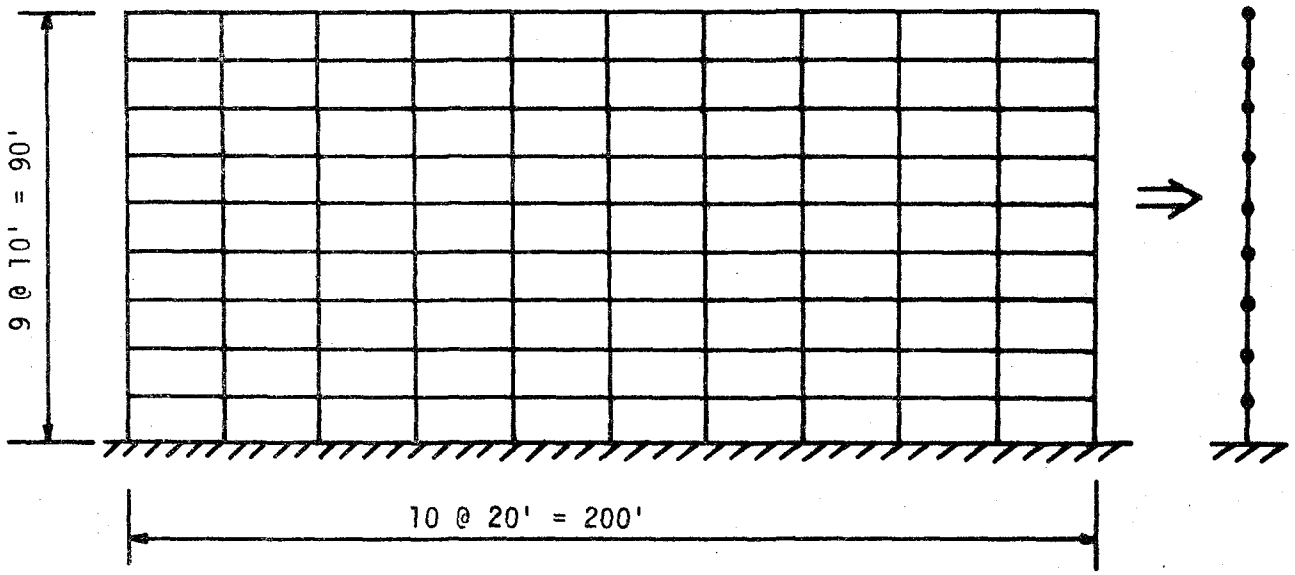

$E = 432000$, $\rho = 1.0$

$A_c = A_g = 3.0$, $I_c = I_g = 1.0$ for all members

(units: ft, kip)

Figure 7 Example 1

The effective shear rigidity for both the models at the ground level is obtained as

$$GA = \left(9 \times \frac{48}{7} + 2 \times \frac{60}{11}\right) \frac{EI_c}{L_c^2} = 3.137 \times 10^5 \text{ kips} \tag{53}$$

The rest have the effective shear rigidity given by

$$GA = (9 \times 4 + 2 \times 2.4) \frac{EI_c}{L_c^2} = 1.762 \times 10^5 \text{ kips} \tag{54}$$

Similarly, the effective bending rigidity for the Timoshenko beam model is obtained as

$$EI = 5.7024 \times 10^{10} \text{ kips - ft}^2 \tag{55}$$

The angular frequencies for the first five modes of vibration obtained by using nine shear beam elements as well as nine Timoshenko beam elements are shown in Table 1. Although the Timoshenko beam model yields a better agreement with the "exact" solution, it should be noted that the shear beam model also proves adequate. In fact the difference between the two approximate solutions is negligible from the practical standpoint. The small discrepancies between the Timoshenko beam model and the shear beam model in this case should be expected as the structure is relatively short as compared to its lateral dimension, and, as a consequence, the gross bending effect is not pronounced.

Fig. 8 shows the first three mode shapes of the Timoshenko beam model, the shear beam model, and the mode shapes of the middle column based on the exact finite element solution. Excellent agreement is noted.

Example 2: 4 Bay - 15 Story Plane Frame

Fig. 9 shows the dimensions and material constants of the structure.

Mode	Exact Frequency	Shear Beam		Timoshenko Beam	
		Frequency	Error %	Frequency	Error %
1	0.7678	0.7687	0.12	0.7685	0.09
2	2.3509	2.2807	-2.98	2.2996	-2.18
3	4.0728	3.7178	-8.71	3.8135	-6.37
4	5.9510	5.0337	-15.41	5.2795	-11.28
5	6.4080	6.1869	-3.45	6.6696	4.08

Table 1 Angular frequencies for the first five modes in Example 1 (rad/sec)

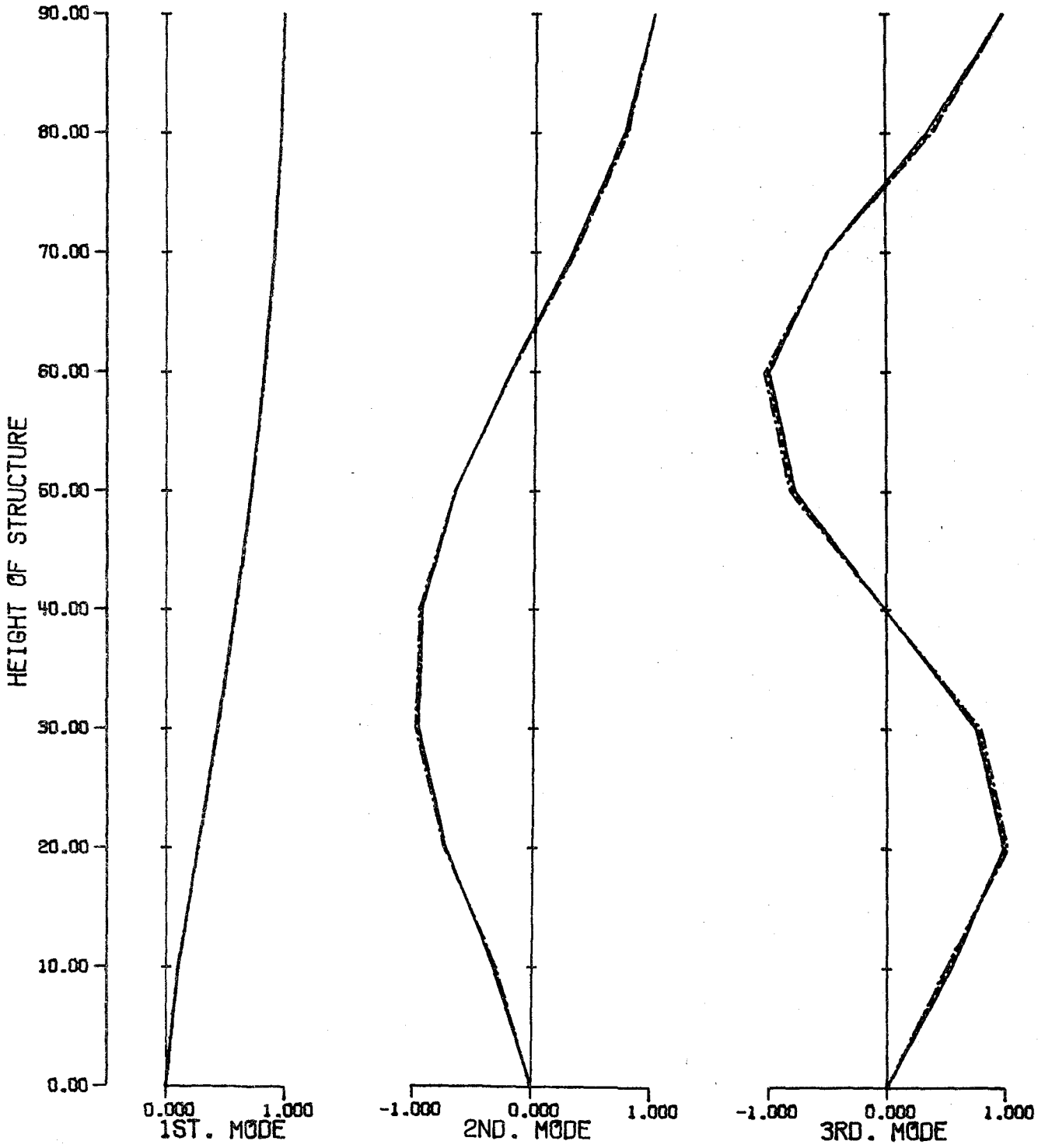

Figure 8 Mode shapes for Example 1 (——— exact, —·—·— shear beam, ----- Timoshenko beam)

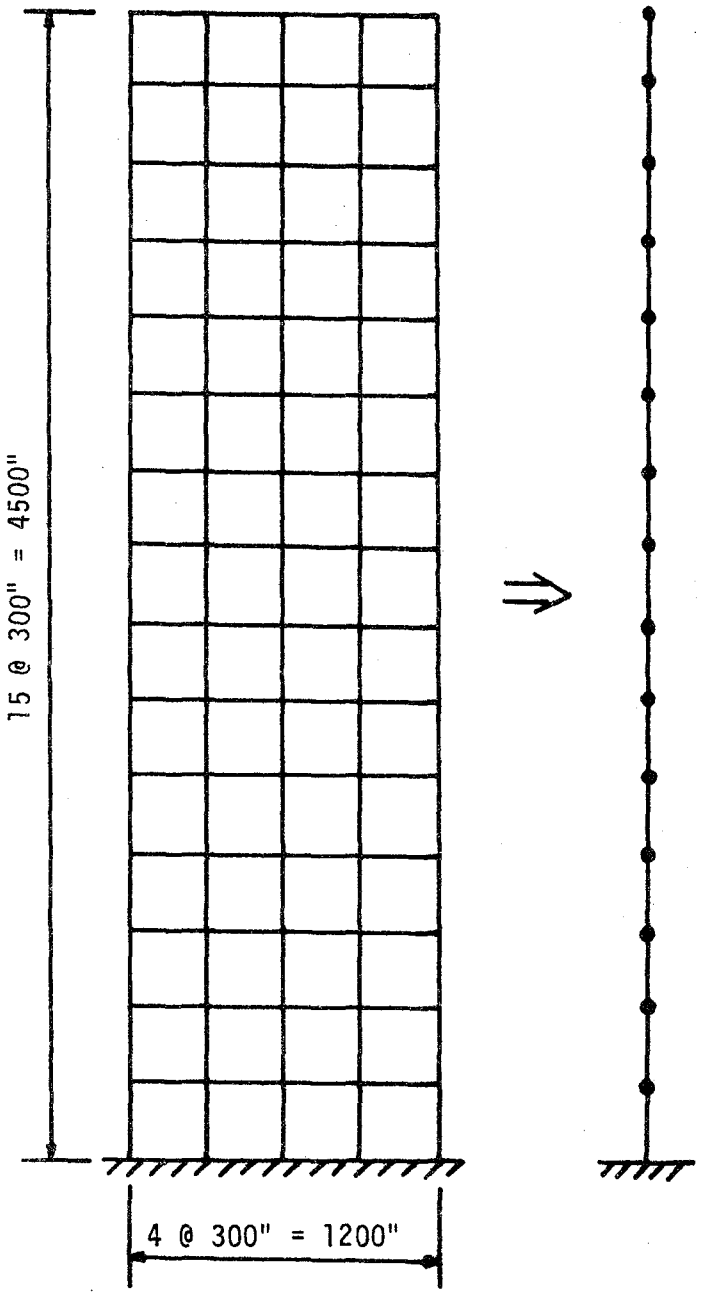

$E = 3.0 \times 10^{7}$, $\rho = 7.45 \times 10^{-4}$

$A_c = A_g = 29.1$, $I_c = I_g = 4000$

(units: in, lb)

Figure 9 Example 2

The floor masses are again lumped at the respective levels as shown in the figure. Fifteen elements are used for both shear beam model and Timoshenko beam model. The angular frequencies for the first five modes are presented in Table 2. The Timoshenko beam solutions are again in close agreement with the exact solutions. It is also expected that the Timoshenko beam model yields more accurate results as the gross bending effect is significant. The shear beam solutions are still quite acceptable as the maximum error stays within 10% from the exact solutions.

One would naturally expect that the frequencies obtained based upon the shear beam model should be higher than those according to the Timoshenko beam model. This, however, is not reflected from the present results in the higher modes. The reason is that the lumped mass system which overestimates the inertia effect especially in the higher modes is employed in the shear beam finite element solution.

In Fig. 10 the mode shapes for the first three modes are shown. Excellent agreement is evident.

Example 3: 4 Bay - 7 Story Plane Frame with Bracings

When bracing is present, the additional stiffnesses due to the braces are calculated according to Eqs. (10) and (30). For the braced frame structure shown in Fig. 11 the floor masses are lumped at each level; and the brace masses are divided equally between two adjacent floors. The simplified structure that is modeled by either shear beam or Timoshenko beam finite elements is also shown. The first five angular frequencies are presented in Table 3, and the first three mode shapes are shown in Fig. 12. It should be pointed out that the third mode is a longitudinal mode and cannot be accounted for by either the shear beam model or the Timoshenko beam model.

Mode	Exact Frequency	Shear Beam		Timoshenko Beam	
		Frequency	Error %	Frequency	Error %
1	4.26	4.68	9.86	4.31	1.2
2	13.08	14.00	7.01	13.16	0.6
3	23.18	23.15	-0.10	23.02	-0.7
4	33.03	32.04	-3.00	32.34	-2.1
5	43.32	40.55	-6.40	41.70	-3.7

Table 2 Angular frequencies for the first five modes in Example 2 (rad/sec)

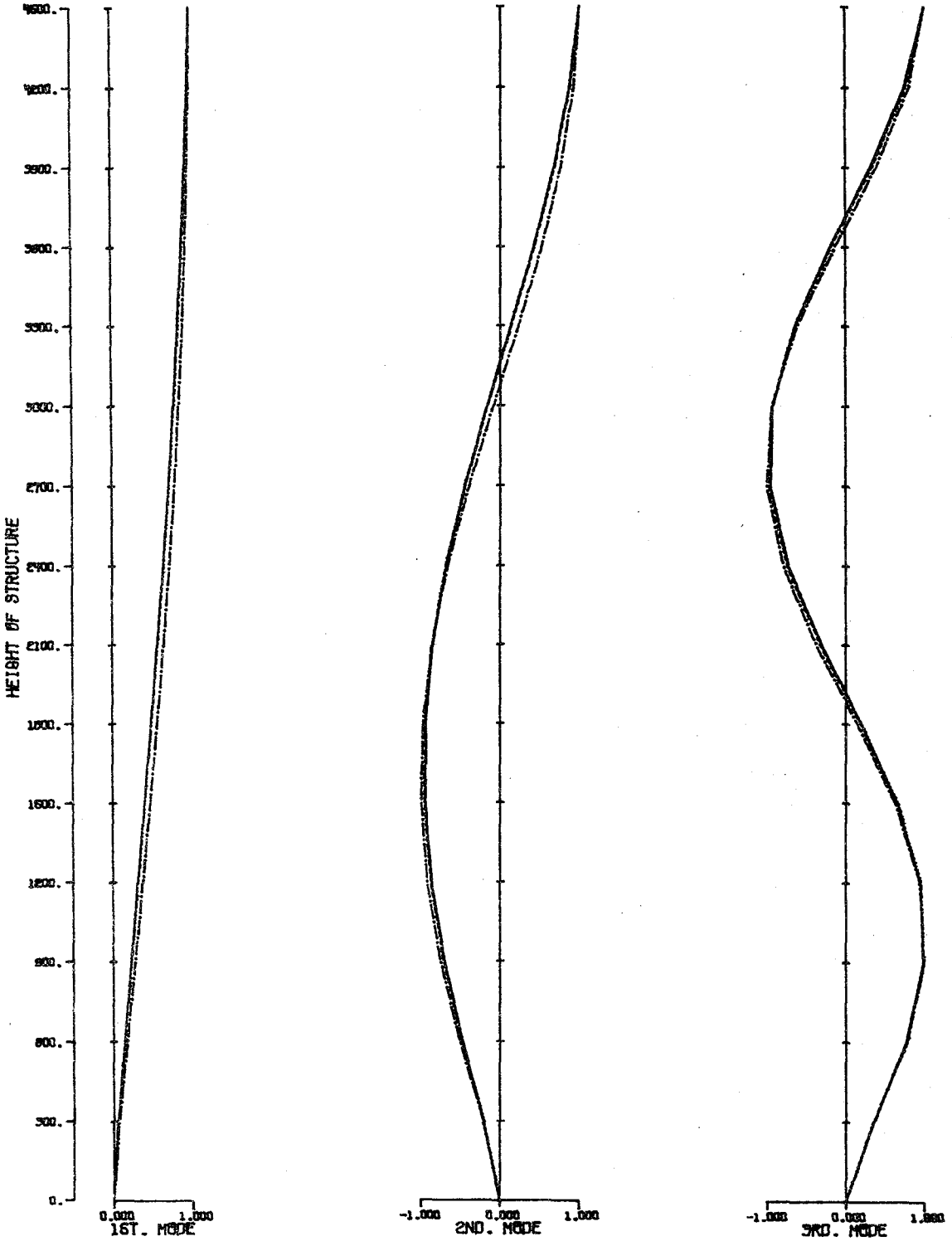

Figure 10 Mode shapes for Example 2 (——— exact, —·—·—· shear beam, ----- Timoshenko beam)

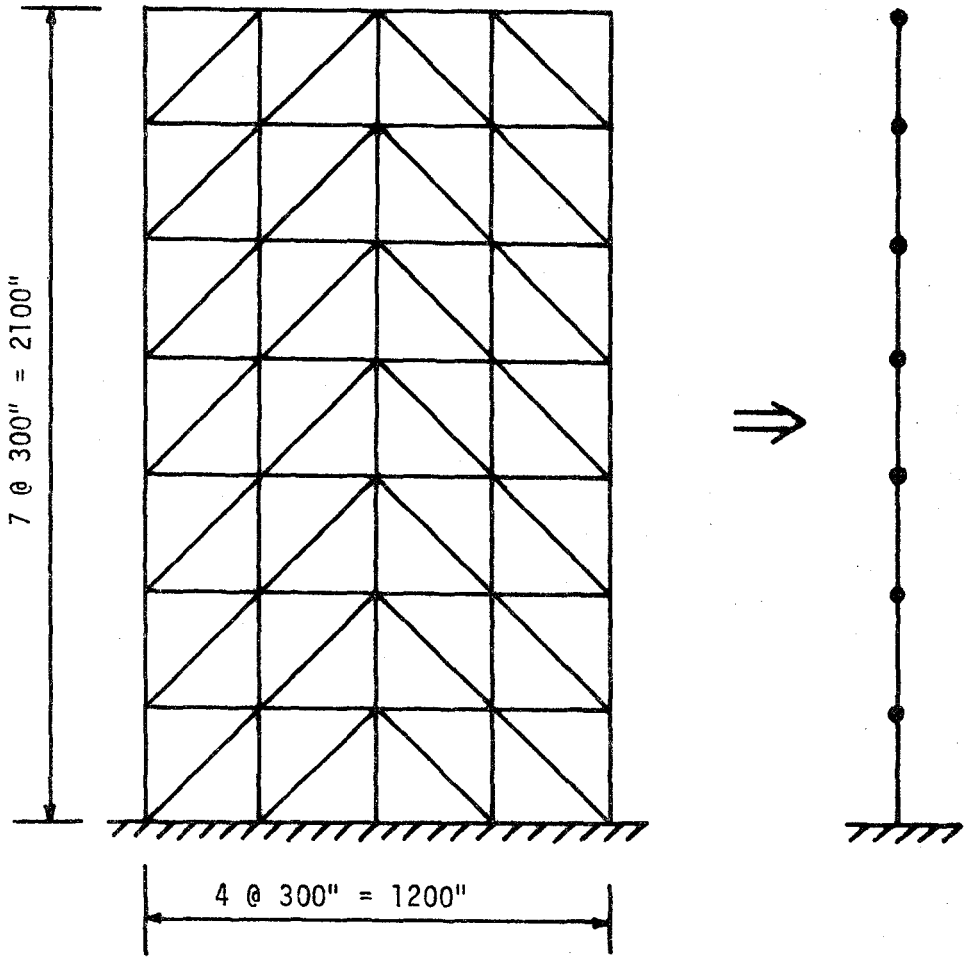

$E = 3.0 \times 10^{7}$, $\rho = 7.45 \times 10^{-4}$

$A_c = A_g = 29.1$, $I_c = I_g = 4000$

$A_b = 5$

(units: in, lb)

Figure 11 Example 3

Mode	Exact Frequency	Shear Beam		Timoshenko Beam	
		Frequency	Error %	Frequency	Error %
1	22.18	24.82	11.9	21.95	-0.8
2	62.73	73.06	16.5	66.56	6.2
3	105.13			105.32	0.2
4	110.62	117.40	6.1	119.02	7.6
5	131.56	155.91	18.5	163.31	24.2

Table 3 Agnular frequencies for the first five modes in Example 3 (rad/sec). The third mode frequency in Timoshenko beam is obtained by considering the structure as an axial member with efficient axial rigidity given in Eq. (56).

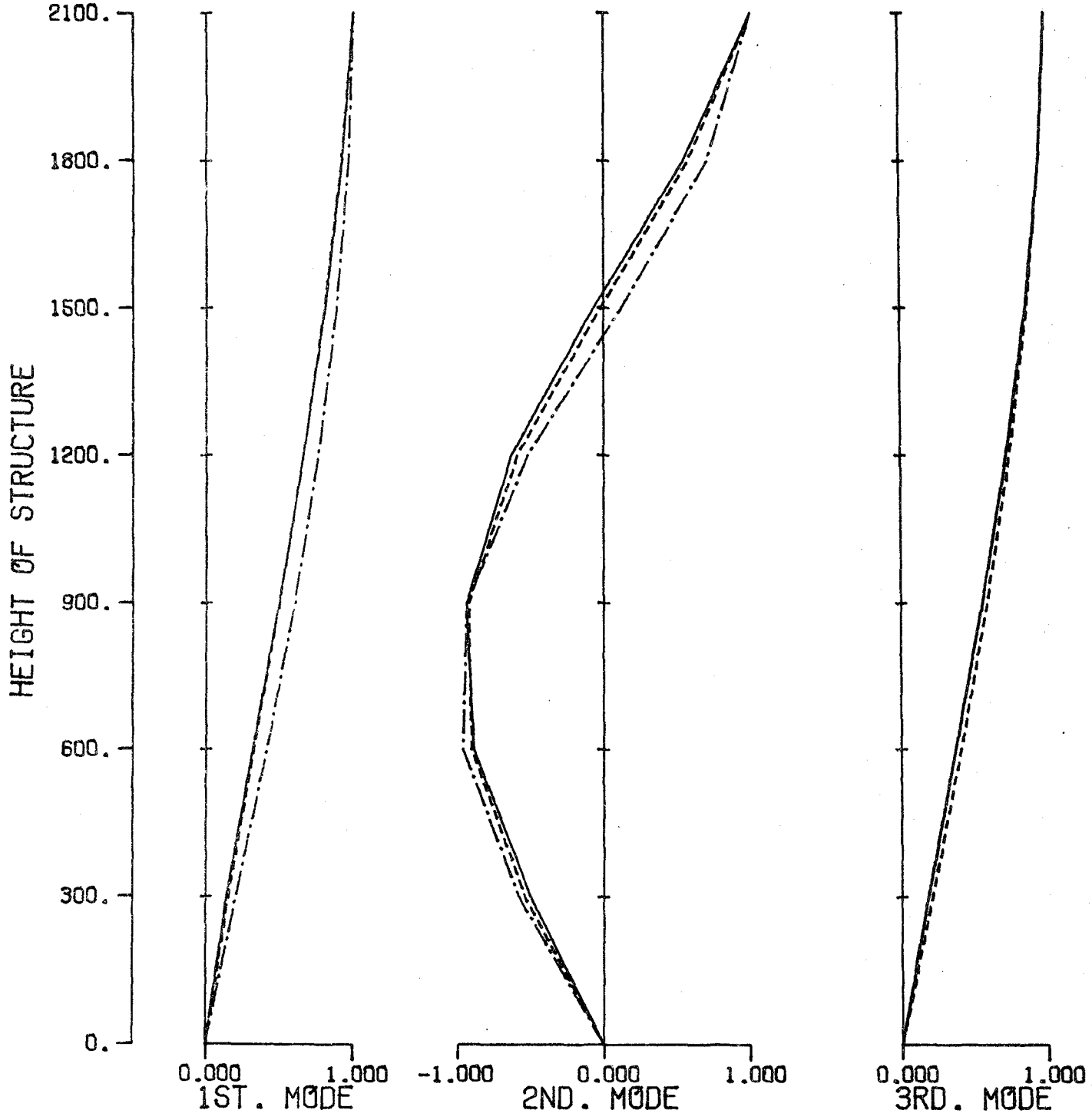

Figure 12 Mode shapes for Example 3 (—— exact, —·—·—· shear beam, ---- Timoshenko beam). The third mode is a longitudinal mode and the amplitude indicates vertical displacement.

The result for mode 3 presented in Table 3 is obtained by considering the structure as an axial member with the effective axial rigidity

$$EA = E\sum A_c + E\sum \frac{\beta^3}{(1+\beta^2)^{3/2}} A_b \tag{56}$$

The stiffness matrix of the axial member is the same in form as that for the shear beam except that GA should now be replaced by EA as given by Eq. (56).

As revealed in this example, the longitudinal mode might appear as one of the lower modes in vibration if the structure is heavily braced. In this case, the axial (longitudinal) motion must be also investigated and compared with the results obtained from the Timoshenko beam model.

Example 4: Central Portion of NZ plane Frame of a Power Plant Structure

The central portion of the NZ plane frame of the fossil fuel steam generating plant of Unit #3 of TVA at Paradise, Kentucky is first chosen to examine the applicability of the simple models applying to the practical engineering frame structures. The geometry and the simplified model are shown in Fig. 13. To retain clearness in the figure, a number is assigned to each member for identification. The number above each horizontal member denotes either the beam number in Table 4(a) or the girder number in Table 4(c); the number to the right of each column represents the column number in Table 4(b). The first five frequencies are presented in Table 5 and the first three mode shapes are shown in Fig. 14.

Example 5: NZ Plane Frame of a Power Plant Structure neglecting Bracings

The whole NZ plane frame without bracings of the above-mentioned power plant structure is now taken for vibration analysis. Fig. 15 shows the geometry and the member code numbers in accordance with those numbers in

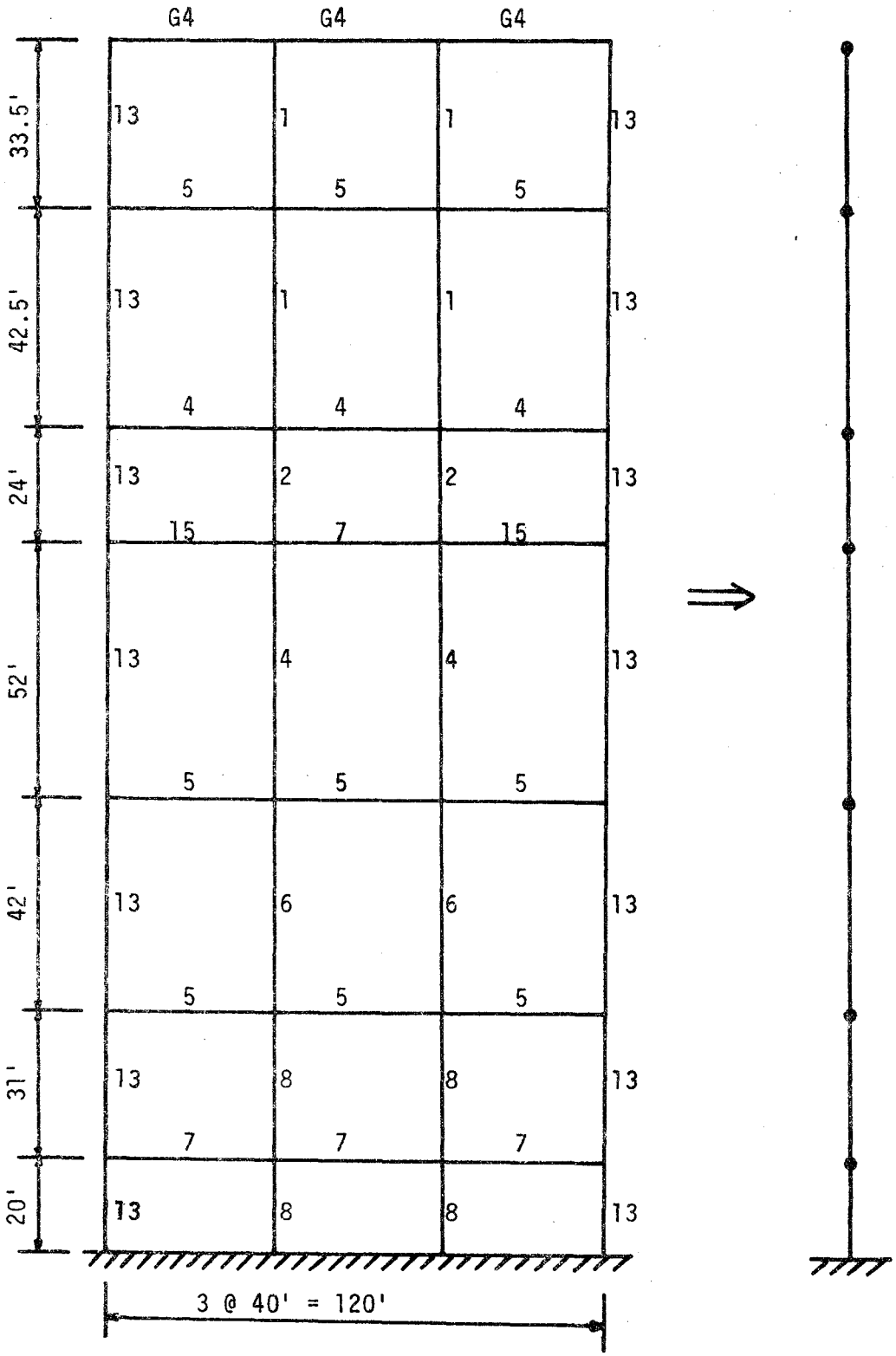

$E = 4.32 \times 10^{6}$, $\rho = 1.5448 \times 10^{-2}$

(units: ft, kip)

Figure 13 Example 4

Beam No.	Designation	Moment of Inertia (FT^4)	Area (FT^2)
1	W 21 x 55	0.05498	0.11250
2	W 21 x 127	0.14564	0.25972
3	W 24 x 68	0.08777	0.13889
4	W 24 x 76	0.10127	0.15556
5	W 24 x 100	0.14468	0.20486
6	W 27 x 94	0.15770	0.19236
7	W 30 x 108	0.21557	0.22083
8	W 30 x 116	0.23775	0.23750
9	W 30 x 124	0.25849	0.25347
10	W 33 x 118	0.28453	0.24167
11	W 33 x 240	0.65586	0.49028
12	W 36 x 135	0.37712	0.27640
13	W 36 x 150	0.43547	0.30694
14	W 36 x 160	0.47068	0.32708
15	W 36 x 170	0.50637	0.34722
16	W 36 x 230	0.72338	0.47014

(a)

Table 4 Member properties for the frame structures in Example 4, 5, 6: (a) beam

Column No.	Designation	Moment of Inertia (FT^4)	Area (FT^2)
1	W 14 x 87	0.01688	0.17778
2	W 14 x 95	0.01852	0.19375
3	W 14 x 111	0.02194	0.22708
4	W 14 x 237	0.05642	0.48403
5	W 14 x 287	0.07089	0.58611
6	W 14 x 314	0.07861	0.64097
7	W 14 x 342	0.08729	0.70139
8	W 14 x 370	0.09597	0.75694
9	W 14 x 426	0.11381	0.86806
10	W 14 x 455	0.12346	0.93056
11	W 14 x 550	0.15721	1.12500
12	W 14 x 605	0.17747	1.23611
13	W 14 x 730	0.22762	1.49310
14	W 21 x 55	0.00233	0.11250
15	W 21 x 62	0.00277	0.12708
16	W 21 x 112	0.01529	0.22917

(b)

Table 4 cont. (b) column

Girder No.	Designation	Moment of Inertia (FT^4)	Area (FT^2)
G1	A	0.72156	0.83333
G2	B	0.78042	0.53646
G3	C	0.45598	0.31250
G4	D	25.31100	1.79170

(c)

Bracing No.	Designation	Area (FT^2)
1	W 10 x 77	0.15764
2	W 12 x 40	0.08194
3	W 12 x 65	0.13264
4	W 12 x 72	0.14722
5	W 12 x 79	0.15764

(d)

Table 4 cont. (c) girder; (d) bracing

Mode	Exact Frequency	Shear Beam		Timoshenko Beam	
		Frequency	Error %	Frequency	Error %
1	1.829	1.882	2.68	1.906	4.29
2	5.296	5.356	1.12	5.605	5.83
3	10.430	9.173	-12.05	10.318	-1.07
4	17.046	13.418	-21.28	15.506	-9.04
5	19.783	17.684	-10.61	19.511	-1.37

Table 5 Angular frequencies for the first five modes in Example 4 (rad/sec)

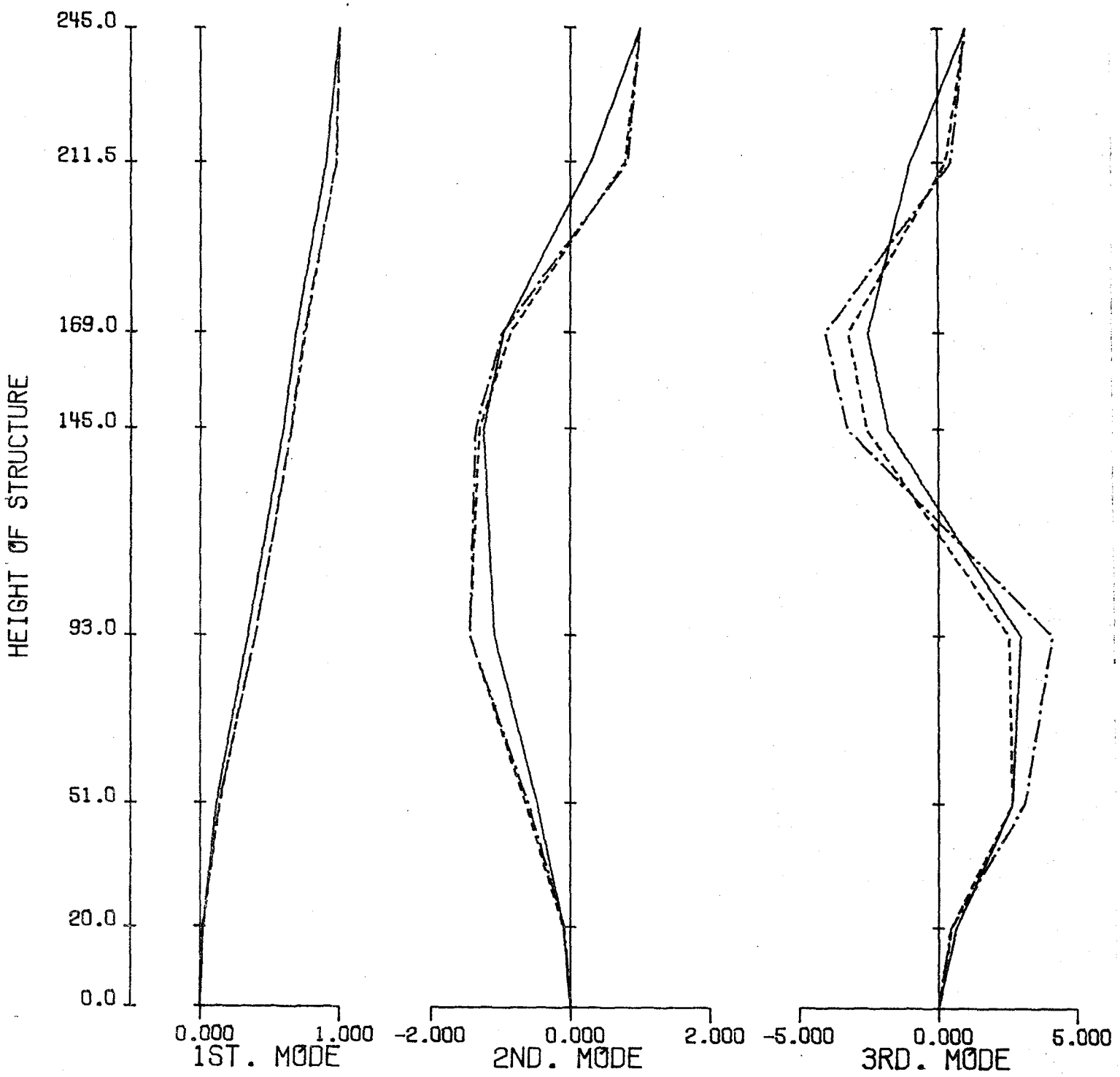

Figure 14 Mode shapes for Example 4 (—— exact, —·—·—· shear beam, ----- Timoshenko beam)

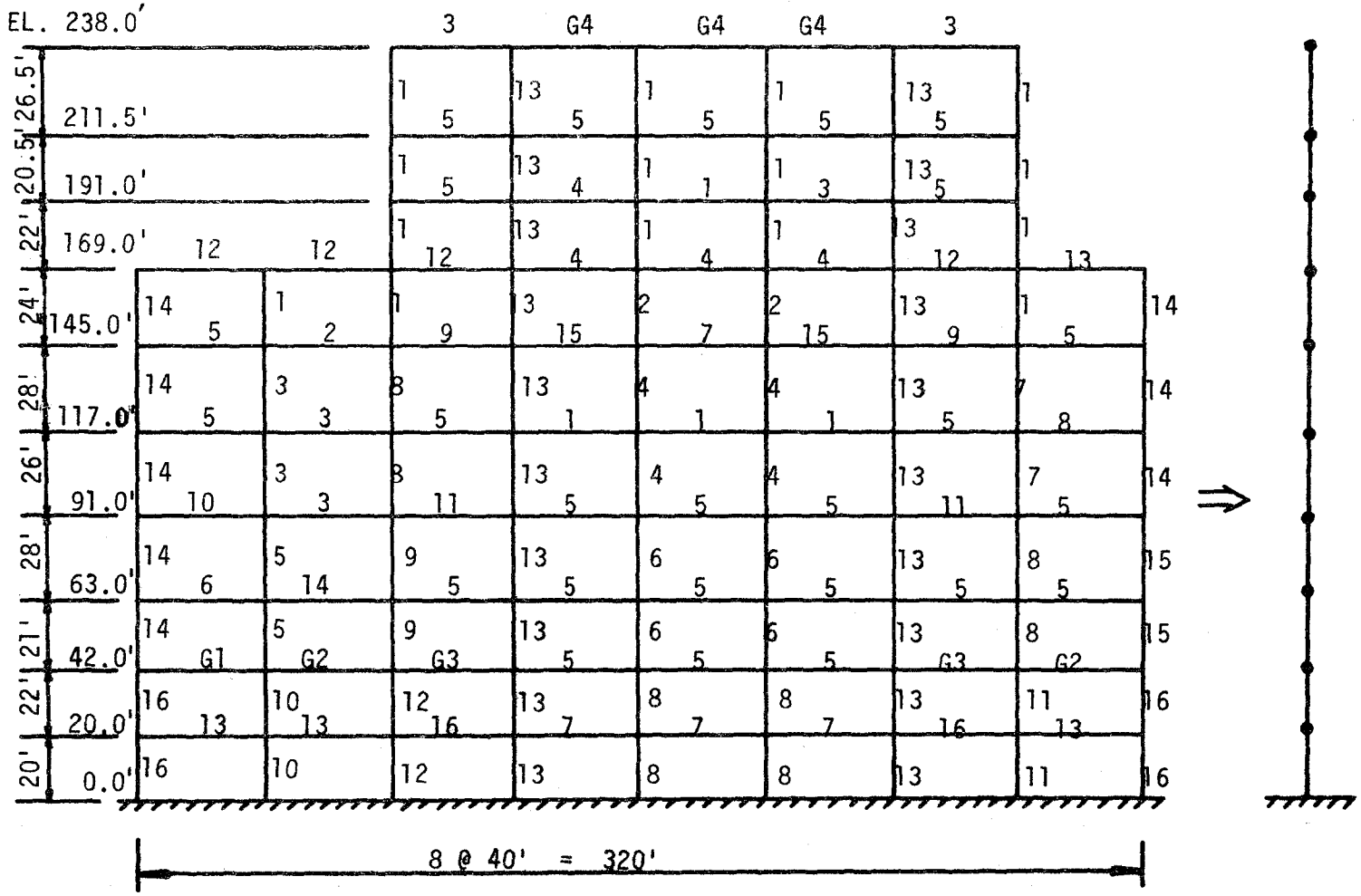

$E = 4.32 \times 10^{6}$, $\rho = 1.5448 \times 10^{-2}$

(units: ft, kip)

Figure 15 Example 5

Table 4. The "simplified" model is also shown in the same figure. Solutions for the first five angular frequencies are given in Table 6. Excellent results for the shear beam model can be expected as the structure behaves as shear-type motion. The Timoshenko beam solutions are also quite acceptable as the maximum error stays within 4% from the exact solutions. Fig. 16 shows the excellent agreement for the first three mode shapes. Thus, the simple models could be fairly accurate even for non-homogeneous frame structures.

Example 6: NZ Plane Frame of Power Plant Structure with Bracings

The same plane frame structure in Example 5 is again considered in this example but with bracings in some selected panels. Fig. 17 shows the same configuration of framework as Fig. 15 plus the location and member code number of each brace. The material constant for each brace is given in Table 4(d). The corresponding "simplified" model is also shown. Due to the uneven distributed bracings at the two outside bays, local bending effects are appreciable in these two bays. The modification process for evaluating the modified shear rigidity GA described in Sec. 9 should be employed. The numerical values of the shear strains ξ, η, and γ must be known so that Eq. (50) can be applied. However, it is unlikely to know these values before the vibration analysis is performed. The static analysis for the substructures of these two outside bays with linearly distributed loading are first carried out separately, and the numerical values for the shear strains ξ, η, and γ are then established. The modified effective shear rigidities for those panels where the local bending effects are significant are then evaluated according to Eq. (50). The simple model analysis procedure is subsequently followed to accomplish the analysis.

Mode	Exact Frequency	Shear Beam		Timoshenko Beam	
		Frequency	Error %	Frequency	Error %
1	3.3715	3.4157	1.31	3.4332	1.83
2	8.7446	8.9710	2.59	9.0627	3.64
3	14.598	14.474	-0.85	14.923	2.23
4	21.754	21.154	-2.76	22.213	2.11
5	26.851	25.254	-5.95	27.455	2.50

Table 6 Angular frequencies for the first five modes in Example 5 (rad/sec)

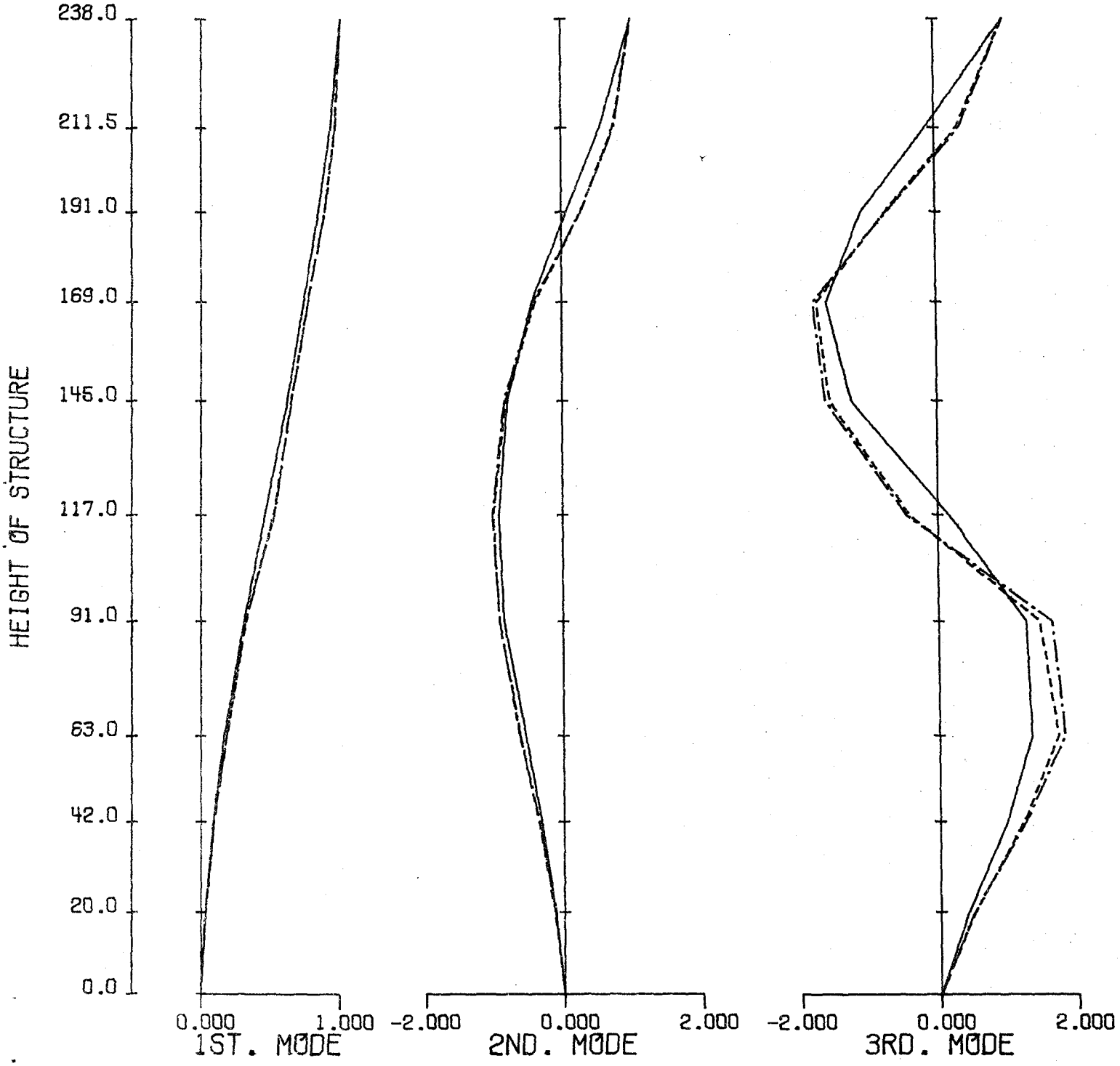

Figure 16 Mode shapes for Example 5 (—— exact, —·—·—· shear beam, ---- Timoshenko beam)

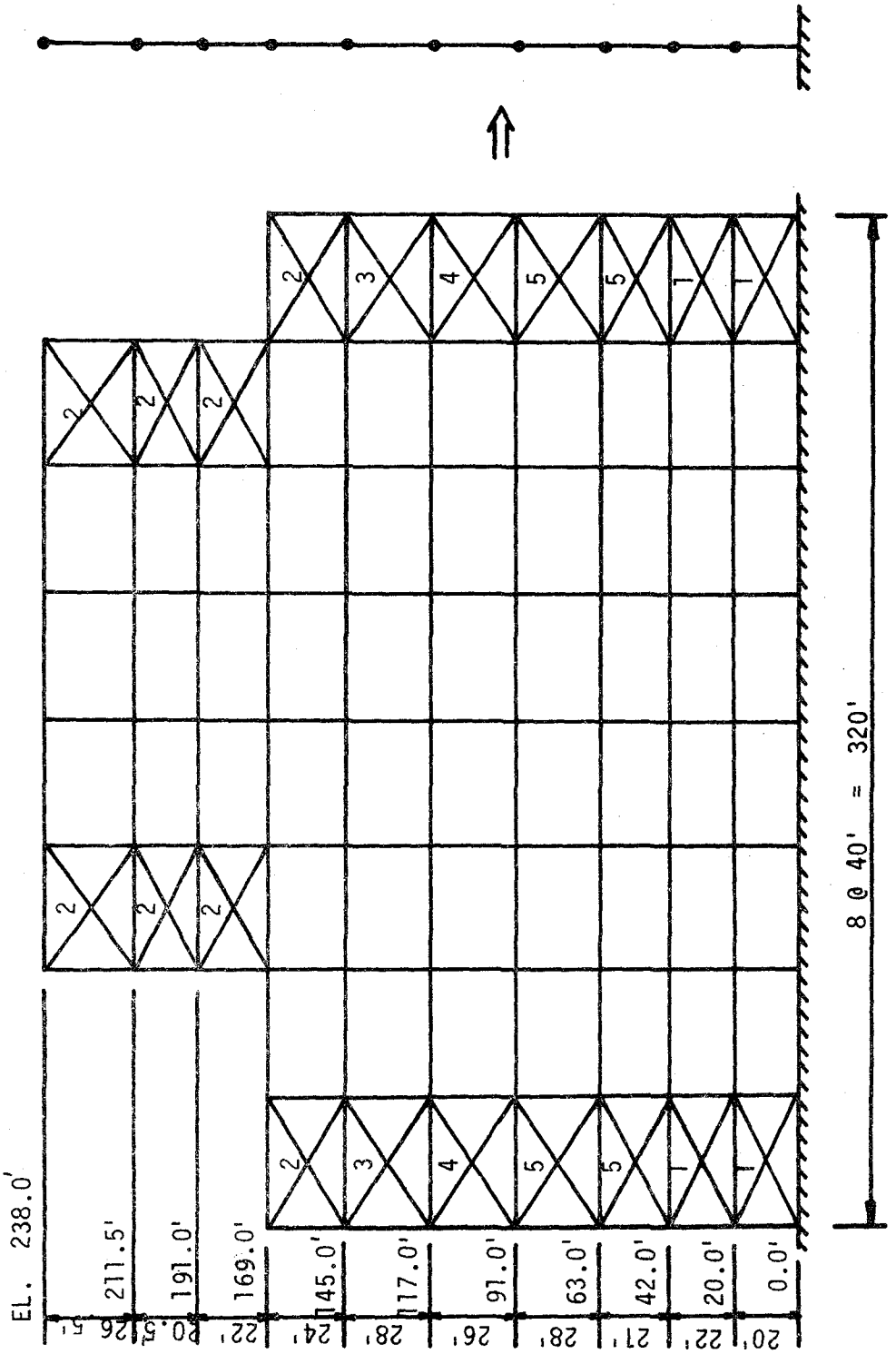

$E = 4.32 \times 10^{6}$, $\rho = 1.5448 \times 10^{-2}$

(units: ft, kip)

Figure 17 Example 6

The first five angular frequencies are shown in Table 7 with 5% of error for the first mode. Fig. 18 shows the first mode shapes of the shear beam model, Timoshenko beam model, and the middle column based upon the finite element solutions. Excellent agreement is noted.

Example 7: The total system of the Power Plant

The simple models are now ready to apply to the total system of the power plant for solutions. The total system contains the steam generator and the supporting frame structure in three-dimensional sense. The supporting frame structure consists of 1412 beam and column elements, 370 diagonal bracing members, two concrete floors, and 611 joints. The two concrete slabs with 8 inches thickness are distributed over some portions of the floors at the elevations of 42 feet and 109 feet above ground, respectively. All the cross bracing members are placed in some selected vertical panels to provide additional lateral resistance against earthquake motion. A three-dimensional outside view of the steel frame structure is depicted in Fig. 19. The detailed geometry and material constants for the members are obtained from the blue prints provided by TVA. The lumped mass model for the steam generator is presented in Table 8. In this analysis, the relative motion of the steam generator against the steel frames is neglected.

The procedures stated in Sec. 10 are now used to model the total system of the power plant in simple beam models for motions in the two principal planes, i.e. x-z and y-z planes. The "simplified" structure is shown in Fig. 20. The number at each node denotes the nodal point number while the number in the parentheses designates the member. The gross effective shear rigidity and gross cross-sectional area for each shear beam

Mode	Exact Frequency	Shear Beam		Timoshenko Beam	
		Frequency	Error %	Frequency	Error %
1	8.647	8.184	-5.35	8.228	-4.84
2	29.508	22.882	-22.5	23.454	-20.5
3	43.564	39.203	-10.0	41.045	-5.78
4	69.933	54.297	-22.4	59.136	-15.4
5	72.200	67.885	-5.98	71.826	-0.52

Table 7 Angular frequencies for the first five modes in Example 6 (rad/sec)

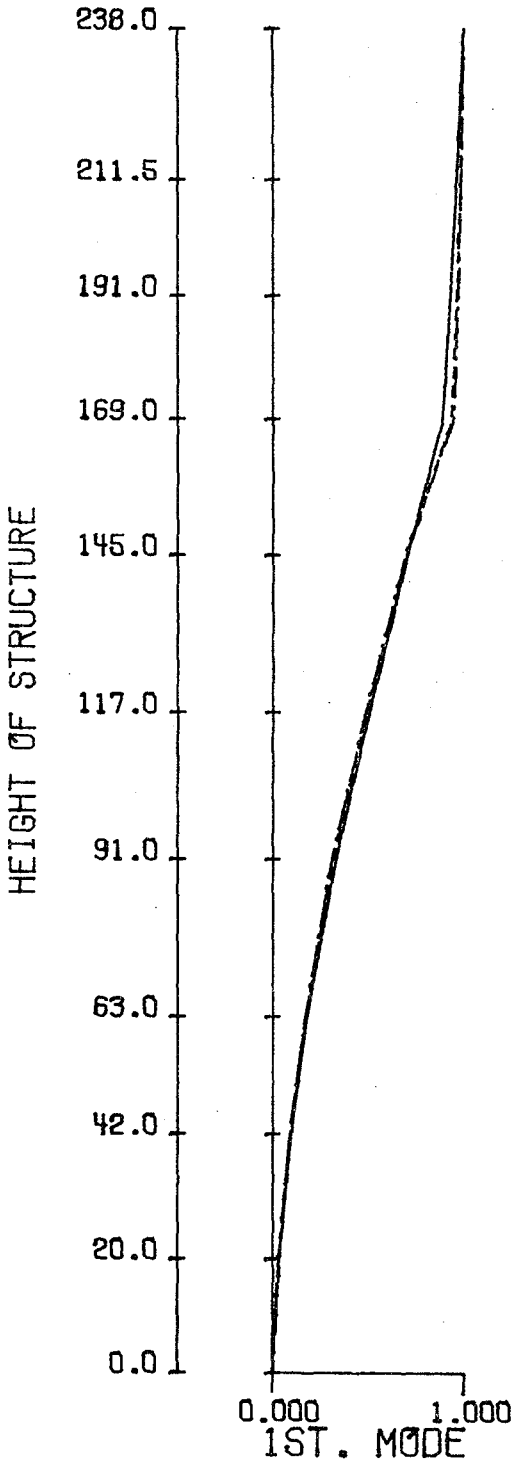

Figure 18 First mode shapes for Example 6 (—— exact, —·—·—· shear beam, ---- Timoshenko beam)

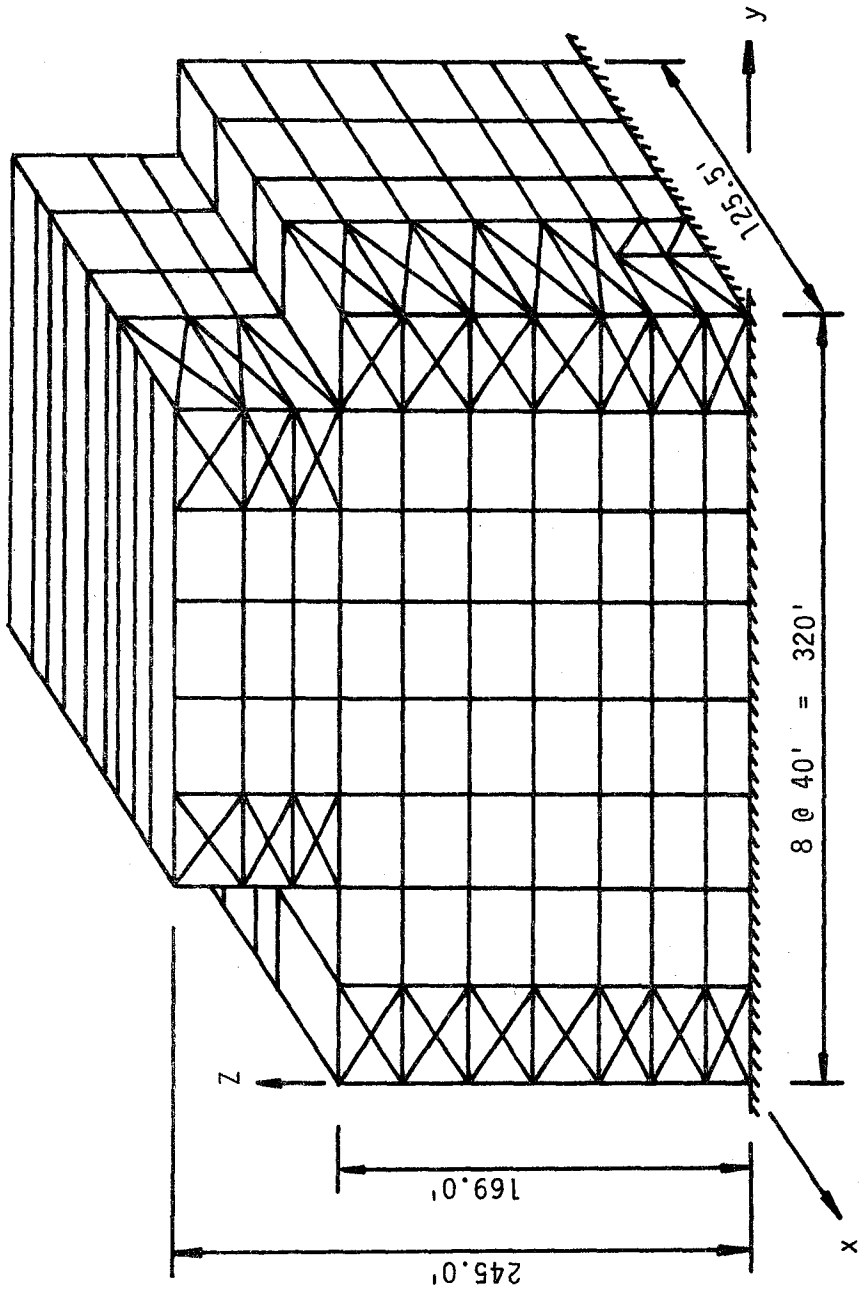

Figure 19 A three-dimensional outside view of the steel supporting frame structure

Z - Ordinate Measured from EL. 0.0	Mass (kips-sec^2/ft^4)
202.0'	187.721
191.0'	70.050
173.0'	42.146
155.0'	121.118
132.0'	16.646
127.0'	129.455
117.0'	13.168
101.6'	5.764
81.5'	65.714
42.0'	100.124

Table 8 Lumped mass distributions for the system generator in Example 7

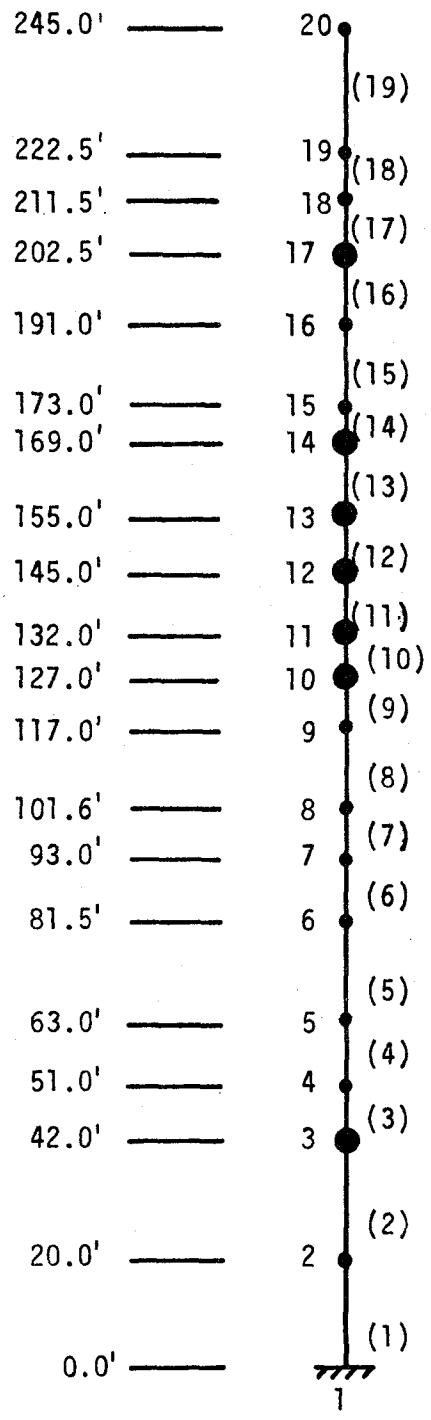

Figure 20 Shear beam model for the total system of the power plant

finite element together with the gross lumped mass at each nodal point are tabulated in Table 9. The natural frequencies for the two flexural modes in x-z and y-z planes, respectively, and the corresponding "exact" solutionsare presented in Table 10. The exact solutions in Table 10 are given by [10] which were obtained by using finite elements with nearly three thousand degrees of freedom. Both frequencies according to the simple shear beam model are in good agreement with the exact solutions. It should be pointed out that in the calculation, only 10 degrees of freedom are used. The mode shapes for the second mode are shown in Fig. 21. The exact mode shape depicts the deformed shape of a typical column in the structure. No exact mode shape for the first mode is available.

The present simple model can only account for the in-plane flexural motion but not the gross torsional vibration. It is known that in highly unsymmetric space frame or truss structures, these two motions are coupled. A more sophisticated simple model that includes both flexural and torsional modes is thus needed.

12. Seismic History Responses Using Simple Models

In this section, time history responses of structures subjected to dynamic loadings are analyzed by using the simple models. In such dynamic analysis, the use of simple models proves to be even more economical in computing time as compared with the use of full scale finite element analysis. In the following, the formulation of the earthquake-response analysis is first derived using the Timoshenko beam model. The shear beam model formulation can be easily derived by suppressing the undesired degrees of freedom, i.e., those variables except the transverse displacement.

Member	Shear rigidity in x-z (kips)	Shear rigidity in y-z (kips)	Area (FT^2)	Mass ($kips\text{-}sec^2/FT^4$)	Node
1	4003971.4	4576087.9	39.818	11.760	2
2	3477758.3	4129643.0	37.704	213.769	3
3	2857812.0	3936786.1	28.740	0.380	4
4	2857812.0	3945815.1	28.508	6.717	5
5	3102887.8	482806.72	28.508	68.673	6
6	2822340.4	5025534.7	28.508	10.445	7
7	3007530.1	3653410.7	24.403	5.764	8
8	3007530.1	3653410.7	24.403	18.840	9
9	2907220.0	3500489.5	24.212	131.601	10
10	2907220.0	3371731.6	24.212	166.460	11
11	2907220.0	3371731.6	24.212	188.422	12
12	2376509.5	2274084.9	18.530	121.118	13
13	2376509.5	2274084.9	18.530	110.816	14
14	1120388.6	2269361.9	15.447	70.050	15
15	1120388.6	2269361.9	15.447	45.818	16
16	1080205.2	2701431.9	14.046	188.538	17
17	1132278.8	2738776.4	14.046	3.019	18
18	1275077.2	2621895.6	14.046	3.466	19
19	1719483.5	2449510.4	14.046	59.095	20

Table 9 Material properties for Example 8

Mode	Exact Frequency	Shear Beam	
		Frequency	Error %
Flexural (x-z)	0.7136	0.7352	3.03
Flexural (y-z)	0.8246	0.8392	1.77

Table 10 Natural frequencies for the two flexural modes in Example 7 (Hertz)

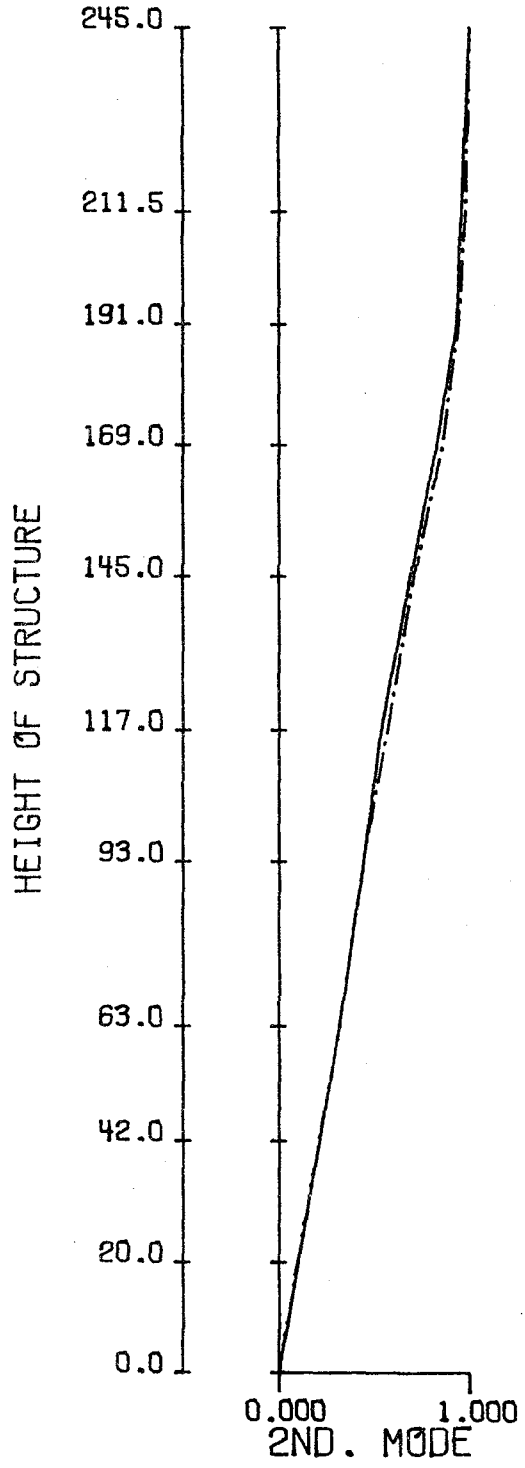

Figure 21 The second mode shapes in y-z plane of Example 7

(—— exact, —·—·—· shear beam)

Consider a multistory frame structure with n stories in height. The structure is first simplified to the simple structure using Timoshenko beam model with the variables v, v', ψ, and ψ' as degrees of freedom at each nodal point. During an earthquake, the simplified structure is excited with a total acceleration $\ddot{v}_i + \ddot{v}_g$ at the i-th story with respect to the reference axis as shown in Fig. 22. Thus the equations of motion of the simplified structure can be written as

$$[M]\begin{Bmatrix} \ddot{v}'_0 \\ \ddot{\psi}'_0 \\ \ddot{v}_1+\ddot{v}_g \\ \ddot{v}'_1 \\ \ddot{\psi}_1 \\ \ddot{\psi}'_1 \\ \vdots \\ \ddot{v}_n+\ddot{v}_g \\ \ddot{v}'_n \\ \ddot{\psi}_n \\ \ddot{\psi}'_n \end{Bmatrix} + [C]\begin{Bmatrix} \dot{v}'_0 \\ \dot{\psi}'_0 \\ \dot{v}_1 \\ \dot{v}'_1 \\ \dot{\psi}_1 \\ \dot{\psi}'_1 \\ \vdots \\ \dot{v}_n \\ \dot{v}'_n \\ \dot{\psi}_n \\ \dot{\psi}'_n \end{Bmatrix} + [K]\begin{Bmatrix} v'_0 \\ \psi'_0 \\ v_1 \\ v'_1 \\ \psi_1 \\ \psi'_1 \\ \vdots \\ v_n \\ v'_n \\ \psi_n \\ \psi'_n \end{Bmatrix} = \{0\} \qquad (57)$$

In Eq. (57), [M], [C], and [K] are the overall mass, damping, and stiffness matrices of order N by N, respectively, in which N equals to 4xn+2 by inserting the boundary conditions $v_0 = 0$ and $\psi_0 = 0$ at the point of support.

The effective earthquake force which produces the dynamic response of this system results from the fact that the inertia-force term in Eq. (57) depends on the total tranverse motion, while the damping and elastic

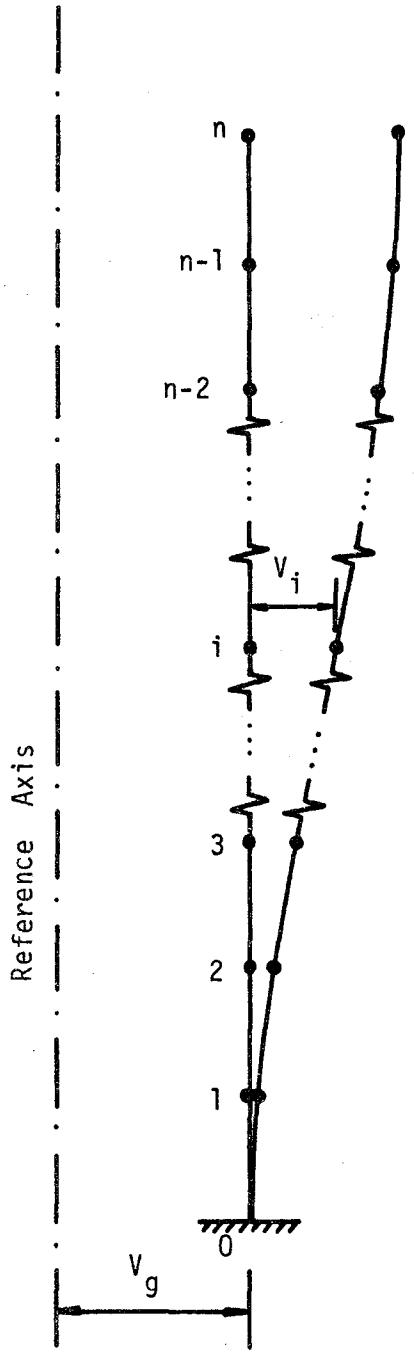

Figure 22 Simplified structure with rigid-base translation

forces depend only on relative motion. With the foregoing, Eq. (57) can be rewritten as

$$[M]\begin{Bmatrix} \ddot{v}'_0 \\ \ddot{\psi}'_0 \\ \ddot{v}_1 \\ \ddot{v}'_1 \\ \ddot{\psi}_1 \\ \ddot{\psi}'_1 \\ \cdot \\ \cdot \\ \cdot \\ \ddot{v}_n \\ \ddot{v}'_n \\ \ddot{\psi}_n \\ \ddot{\psi}'_n \end{Bmatrix} + [C]\begin{Bmatrix} \dot{v}'_0 \\ \dot{\psi}'_0 \\ \dot{v}_1 \\ \dot{v}'_1 \\ \dot{\psi}_1 \\ \dot{\psi}'_1 \\ \cdot \\ \cdot \\ \cdot \\ \dot{v}_n \\ \dot{v}'_n \\ \dot{\psi}_n \\ \dot{\psi}'_n \end{Bmatrix} + [K]\begin{Bmatrix} v'_0 \\ \psi'_0 \\ v_1 \\ v'_1 \\ \psi_1 \\ \psi'_1 \\ \cdot \\ \cdot \\ \cdot \\ v_n \\ v'_n \\ \psi_n \\ \psi'_n \end{Bmatrix} = -\ddot{v}_g\,[M]\begin{Bmatrix} 0 \\ 0 \\ 1 \\ 0 \\ 0 \\ 0 \\ \cdot \\ \cdot \\ \cdot \\ 1 \\ 0 \\ 0 \\ 0 \end{Bmatrix} \qquad (58)$$

or in matrix form:

$$[M]\{\ddot{X}\} + [C]\{\dot{X}\} + [K]\{X\} = -\ddot{v}_g[M]\{1\} \qquad (59)$$

in which $\{1\}$ represents a column of ones occurring at the $3 + 4(i-1)$ th rows where $i = 1, 2, \ldots n$. This vector expresses the fact that a unit static translation of the base of this structure produces directly a unit displacement in the transverse degrees of freedom.

Numerical schemes to obtain the solution to Eq. (59) are numerous. The procedures are, however, mainly divided into two general categories, namely, direct integration and mode superposition [11]. In the direct integration procedure, the step-by-step integration is performed directly on Eq. (59) in its coupled form. As a result, considerably computational work is expected as the scheme is carried out successively at each discrete

time interval Δt. In the modal superposition method, the natural modes of vibration are used to decouple the cequations of motion [12]. Since only a few modes are usually sufficient to ensure an accurate account of the dynamic response, the mode superposition is computation-wise efficient and thus is employed in the present work.

In the mode superposition analysis, it is assumed that the structural response can be described adequately by the p lowest vibration modes, where $p << N$ [13]. In fact, it has been observed that, for most types of loadings, the lower modes dominate the transient dynamic response of the structure [14]. Furthermore, the mathematical idealization of any complex structural system by the simple models also tends to be less accurate in predicting the higher modes of vibration. Therefore the number of modes considered in a dynamic response analysis can be reasonably limited to the first p modes.

It is well known that damping plays an important role in the dynamic response of structures subjected to earthquakes. Generally, in the mode superposition method, damping is assumed to be uncoupled and is given to each mode as a percentage of the critical damping. Therefore a damping ratio can be assigned for each mode based upon experimental data [15].

The procedures of the mode-superposition method are described as follows.

The first P modes are taken to construct the Nxp modal matrix,

$$[\Phi] = [\{\phi\}_1, \{\phi\}_2, \cdots \{\phi\}_p] \tag{60}$$

where $\{\phi\}_i$ (i = 1-p) are the p lowest shape vectors. Introducing the normal co-ordinates defined by the relation

$$\{X\} = [\Phi]\{Y\} \tag{61}$$

and substituting Eq. (61) into Eq. (59), the uncoupled equations of motion, after multiplying with the transposed matrix of $[\Phi]$, have the form

$$[M^*]\{\ddot{Y}\} + [C^*]\{\dot{Y}\} + [K^*]\{Y\} = \{F^*\} \tag{62}$$

where $[M^*]$, $[C^*]$, and $[K^*]$ are the pxp normal (or diagonalized) mass, damping, and stiffness matrices, respectively, and $\{Y\}$ and $\{F^*\}$ are the corresponding pxl normal co-ordinate and force vectors. The individual terms in these matrices are given by

$$\left.\begin{aligned} m_r^* &= \{\phi\}_r^T[M]\{\phi\}_r \\ c_r^* &= \{\phi\}_r^T [C]\{\phi\}_r = 2\, m_r^* \omega_r \xi_r \\ k_r^* &= \{\phi\}_r^T [K]\{\phi\}_r = m_r^* \omega_r^2 \\ f_r^* &= -\ddot{v}_g \{\phi_r\}^T [M]\{1\} \end{aligned}\right\} \quad r = 1, 2, \ldots p \tag{63}$$

where ω_r and ξ_r are the natural frequency and damping ratio of the rth mode of vibration. It should be noted that the damping matrix [C] also possesses the same orthogonal property as the mass and stiffness matrices, i.e.,

$$\{\phi\}_r^T [C]\{\phi\}_s = 0 \quad , \quad r \neq s \tag{64}$$

In Eq. (64), $\{\phi\}_r$ and $\{\phi\}_s$ are the shape vectors of modes r and s, respectively.

The p equations of motion in Eq. (62) are now uncoupled and can be treated individually. Each equation in Eq. (62) has the typical form of second order differential equation with constant coefficient

$$m^*\ddot{Y}(t) + c^*\dot{Y}(t) + k^*Y(t) = f^*(t) \tag{65}$$

or

$$\ddot{Y}(t) + 2\xi\omega\dot{Y}(t) + \omega^2 Y(t) = \frac{1}{m^*} f^*(t) \tag{66}$$

Many numerical integration methods are currently used for solutions to Eq. (66). Among them are the central difference method, the Houbolt method, the Newmark method, and the Wilson θ method, etc. [11]. In this work, the Wilson θ method is adopted because it is optimized with respect to stability and accuracy [16].

The assumption made in the Wilson θ method is that the acceleration varies linearly during the time interval $\theta\Delta t$, where θ is a numerical quantity which is greater than 1.0 to ensure accuracy and stability in the integration. It is recommended that $\theta = 1.4$ be used.

Initial conditions are needed in the finite difference solution. By multiplying Eq. (61) by [M] and $[\Phi]^T$ successively, Eq. (61) becomes

$$[\Phi]^T[M]\{X\} = [\Phi]^T[M][\Phi]\{Y\} \tag{67}$$

The normal co-ordinate $\{Y\}$ can be expressed as

$$\{Y\} = [\Phi]^T[M]\{X\} \tag{68}$$

if the normalization process is applied to the modal matrix $[\Phi]$. At $t = 0$, $X(0) = \dot{X}(0) = \ddot{X}(0) = 0$, and consequently,

$$Y(0) = \dot{Y}(0) = \ddot{Y}(0) = 0 \tag{69}$$

The p solutions of Eq. (66) can be obtained for any given random earthquake records in the transverse direction up to any desired time t. It should be noted that the random earthquake records are linearly interpolated before the numerical integration scheme is employed.

The displacement vector $\{X\}$ of the "simplified" structure can be obtained easily using Eq. (61). Since only the transverse displacement at each story level is of interest, the multiplication process corresponding

to such element in the displacement vector {X} is sufficient to provide the necessary outcome for the transverse displacement.

Dynamic time history responses for the shear beam model can also be easily followed. Instead of four degrees of freedom at each nodal point for the Timoshenko beam model, only one degree of freedom, i.e., tranverse displacement, is retained in the shear beam model.

Solutions for the time history responses of some frame structures are studied in the following by using either the Timoshenko beam model or the shear beam model with or without damping.

A homogeneous 4-Bay, 7-story plane frame structure shown in Fig. 23 in first selected for illustration. The shear beam model is also shown in the same figure. The "complex" frame structure and its "simplified" shear beam structure are then excited, respectively, by the 1940 El Centro N-S earthquake ground acceleration component of 30-second duration as depicted in Fig. 24. The "exact" time history response for the central column of the frame structure together with that of the approximate solution of the simplified shear structure at each story level is then plotted in Fig. 25. Fifteen modes are taken for mode superposition in the exact solutions while four modes are used in simple model solutions. The close agreement shows that the simple shear beam model, in this particular example, yields fairly remarkable results. It is found that the first mode dominates the response. In this case, it is sufficient to take the first few modes for the mode superposition method without appreciable loss of accuracy.

Fig. 26 shows some of the "exact" time history responses together with the simple shear beam model solutions for the NZ plane frame structure shown in Fig. 15 to the 1940 El Centro N-S component with duration

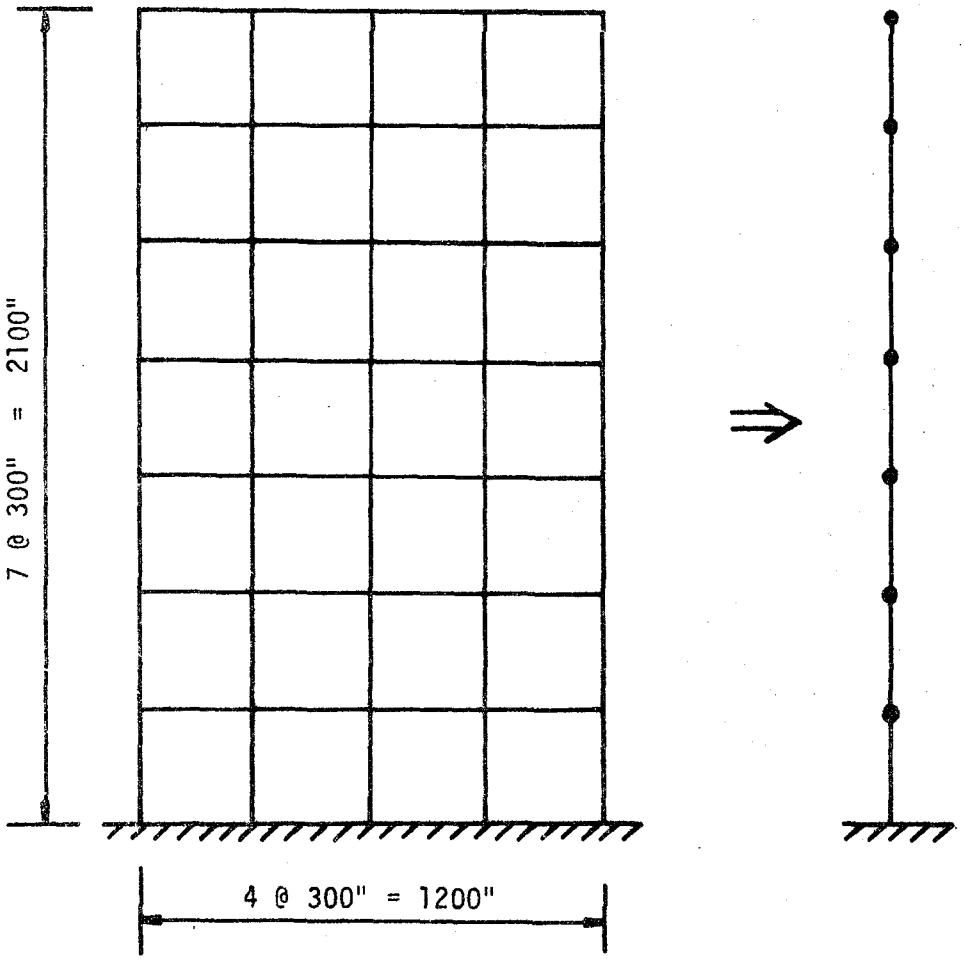

$E = 3.0 \times 10^{7}$, $\rho = 7.45 \times 10^{-4}$

$A_c = A_g = 29.1$, $I_c = I_g = 4000$

(units: in, lb)

Figure 23 Example for time history response analysis

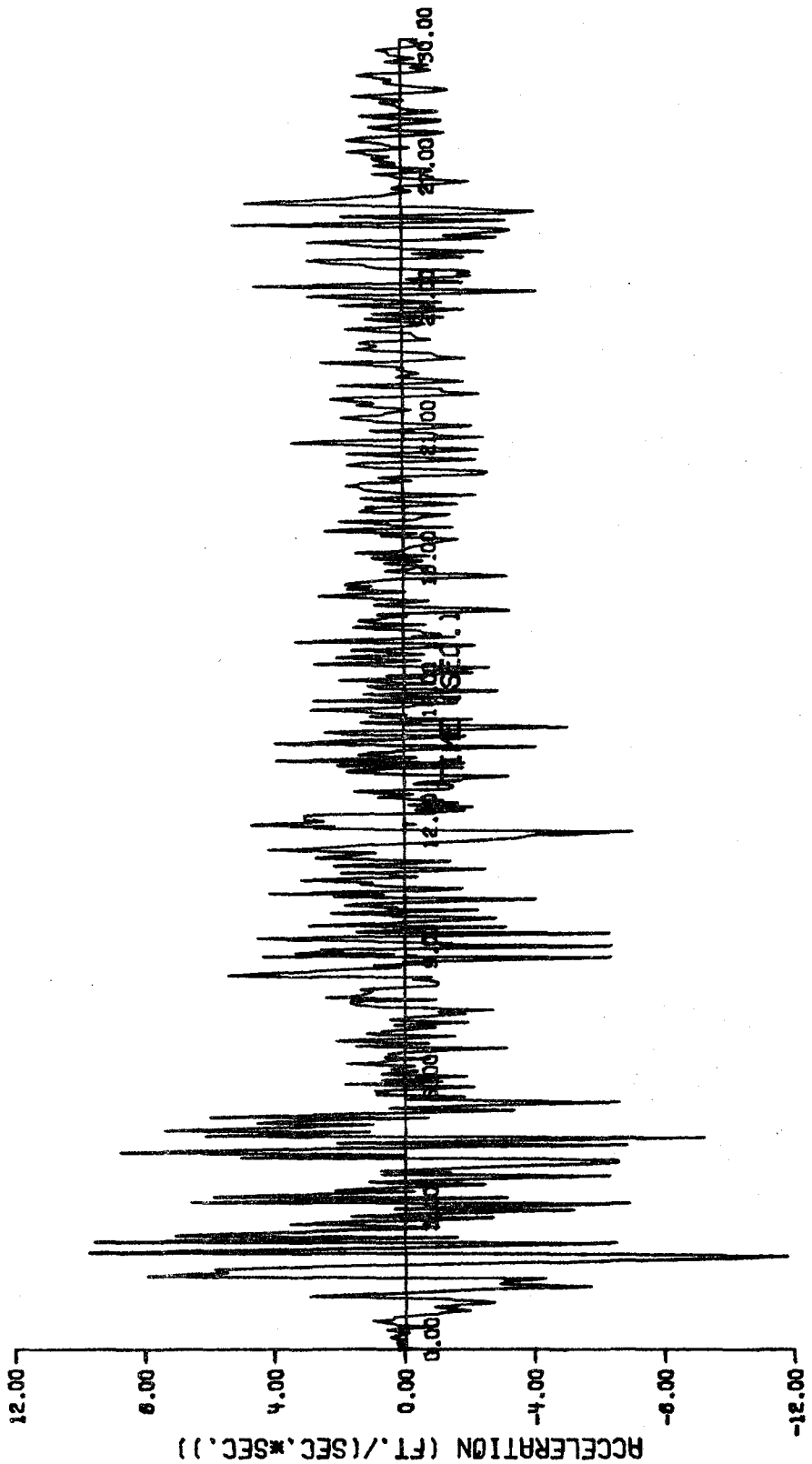

Figure 24 Accelerogram of N-S component for 30-second duration from El Centro Earthquake, May 18, 1940

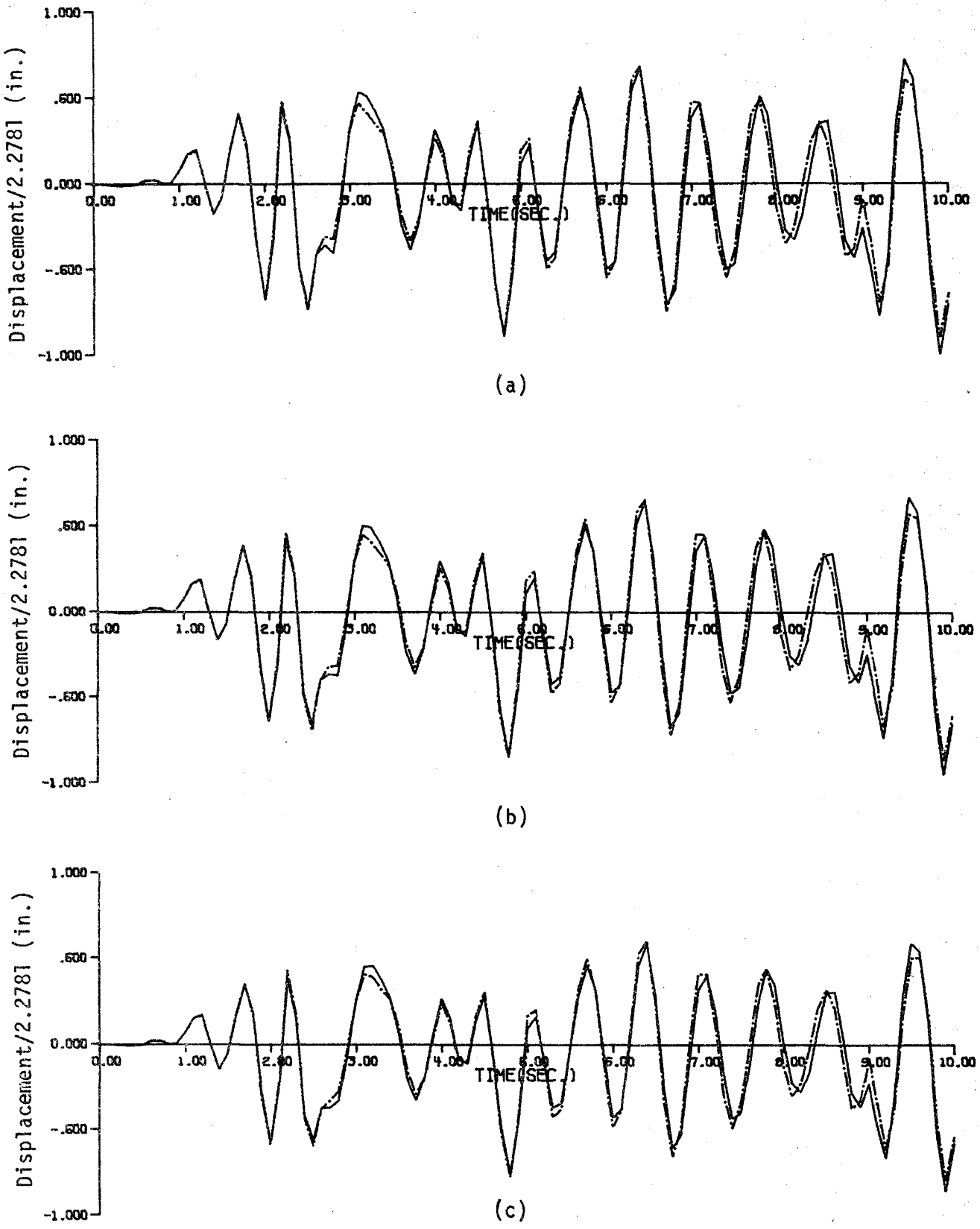

Figure 25 Time history responses(—— exact, —·—·—· shear beam):
(a) the 7th story; (b) the 6th story; (c) the 5th story

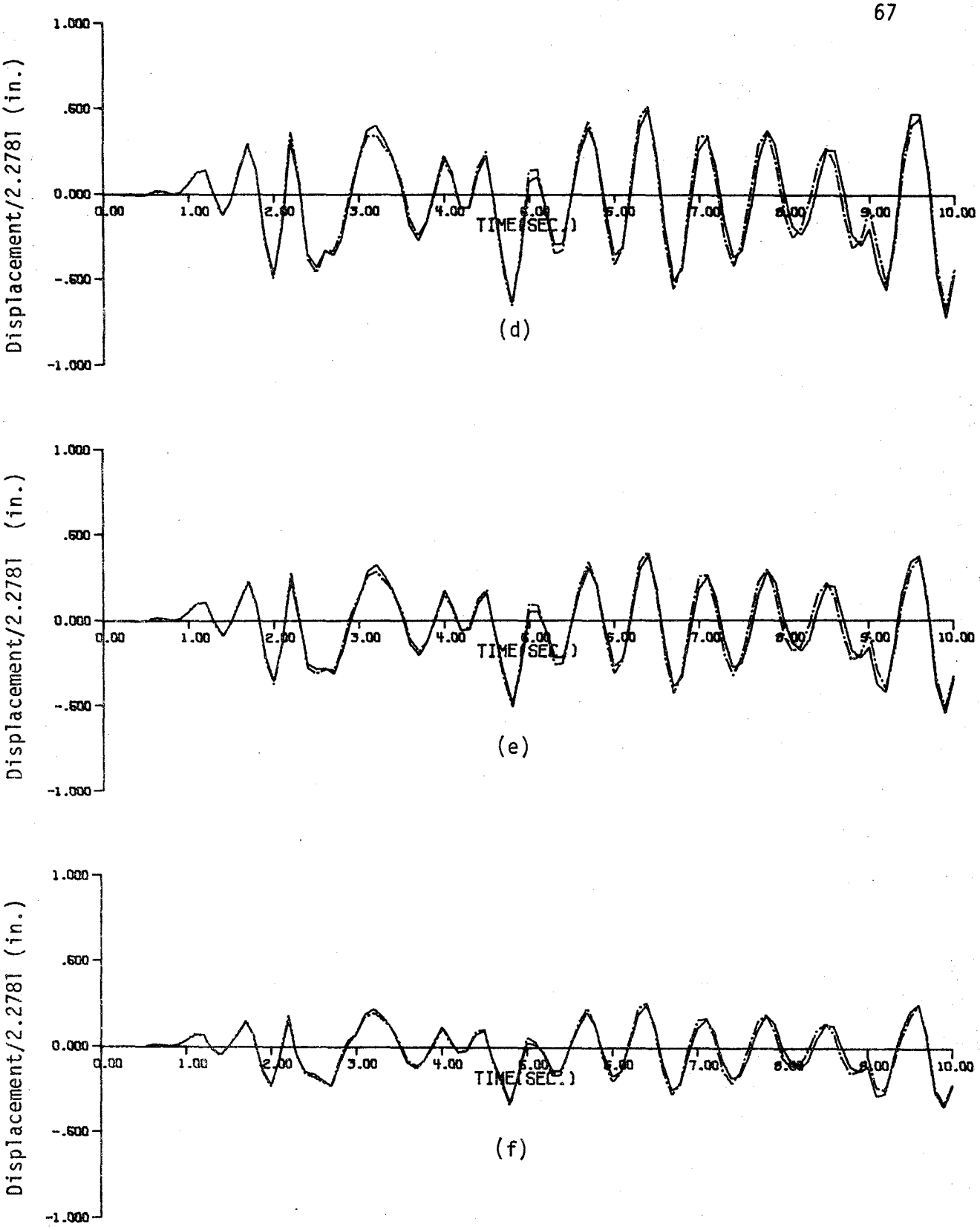

Figure 25 cont. (d) the 4th story; (e) the 3rd story; (f) the 2nd story

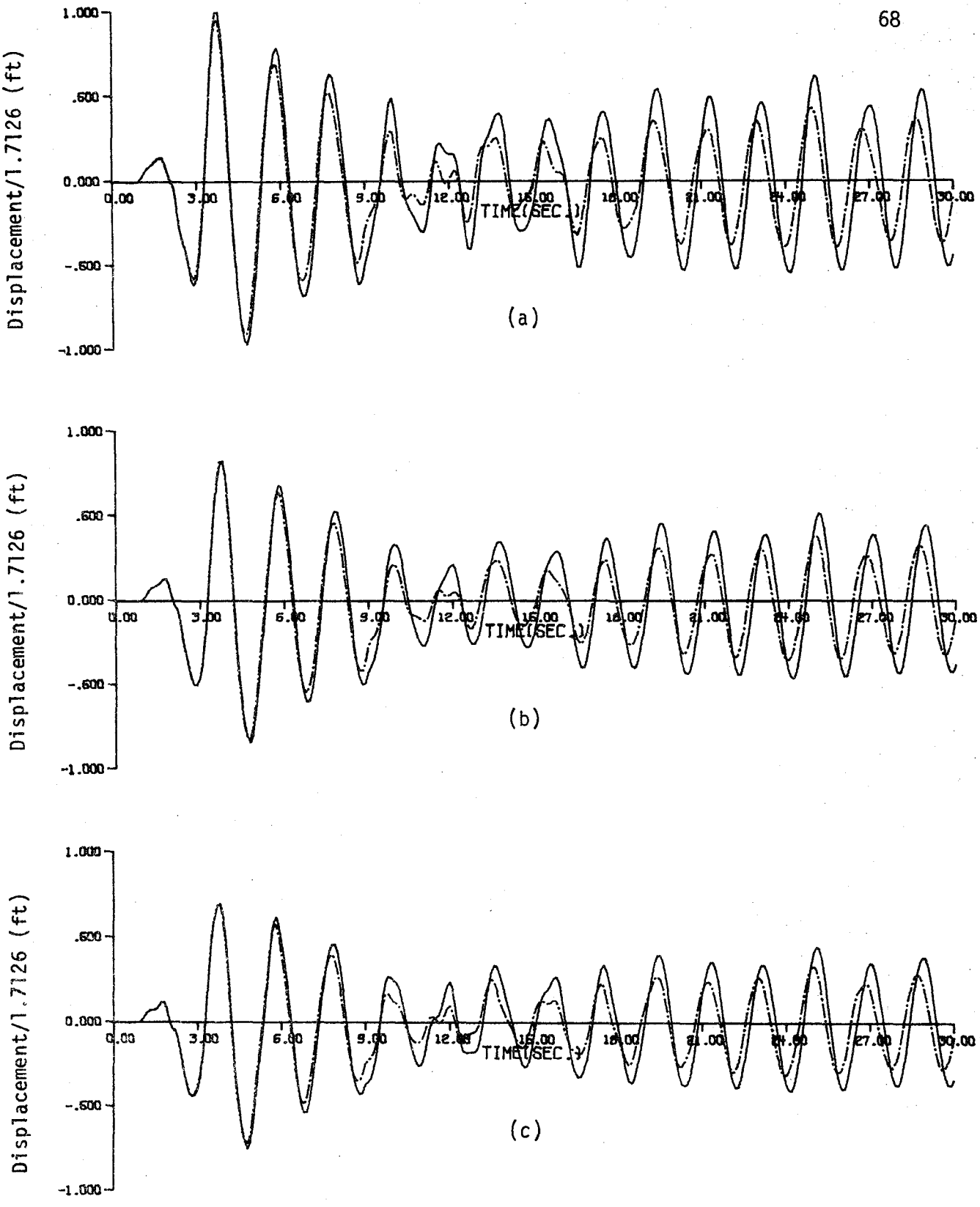

Figure 26 Time history responses (—— exact, —·—·—· shear beam): (a) the 10th story; (b) the 8th story; (c) the 7th story

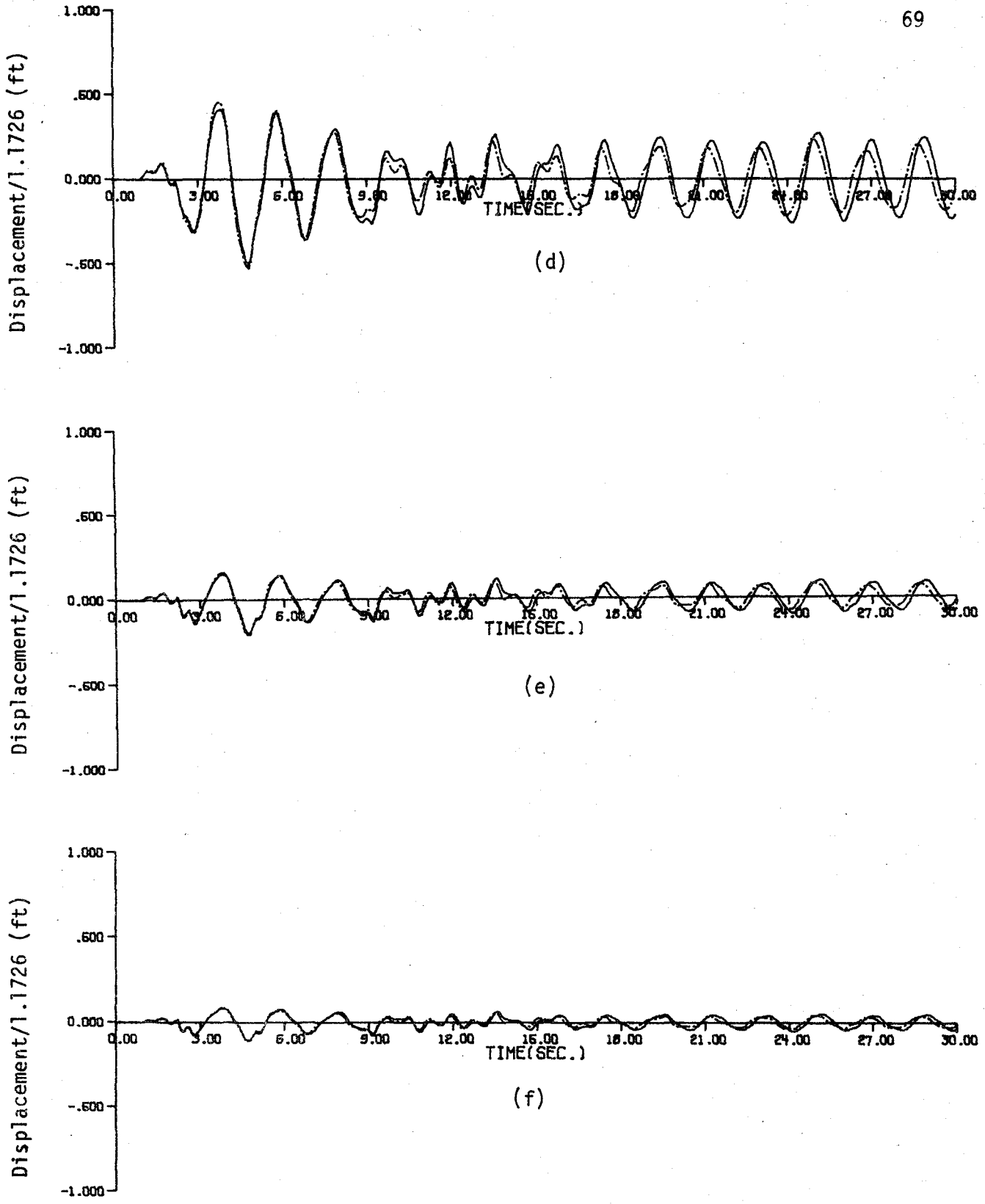

Figure 26 cont. (d) the 5th story; (e) the 3rd story; (f) the 2nd story

of 30 seconds shown in Fig. 24. The maximum displacement is observed at t = 3.80 seconds with magnitude of 1.7126 feet in the last story at elevation of 238.0 feet. It is interesting to note that the higher modes of vibration of a set-back building can make a very substantial contribution to its total seismic response. This fact has been demonstrated in a recent work by Humar and Wright [17]. In this example, ten modes are taken for mode superposition in exact response solutions while five modes are used in simple model solutions. Close agreement is also noted.

The time history responses for structures that have significant gross bending deformations should be computed by using the Timoshenko beam model. Examples with this characteristic are the 4-Bay, 15-Story plane frame structure and the 4-Bay, 7-Story plane frame structure with bracings in Examples 2 and 3, respectively. Figure 27 shows typical time history responses of the shear beam model, the Timoshenko beam model, and the responses of the middle column based upon the exact finite solution for the 4-Bay, 15-Story plane frame structure in Example 2. The 1940 El Centro N-S acceleration component is used as the input of ground motion. Ten modes are used for the exact response solutions and five modes are taken in simple model solutions for mode superposition. Solutions for the 4-Bay, 7-Story plane frame structure with bracings to the same excitation but with 1.5% critical damping are plotted in Fig. 28. In this example, ten modes are also used for the "exact" solutions while only the first two modes are taken for mode superposition in the simple model solutions. Both simple models yield very good solutions.

As a final example in this section, the seismic responses for the total system of the power plant structure shown in Fig. 19 subjected to

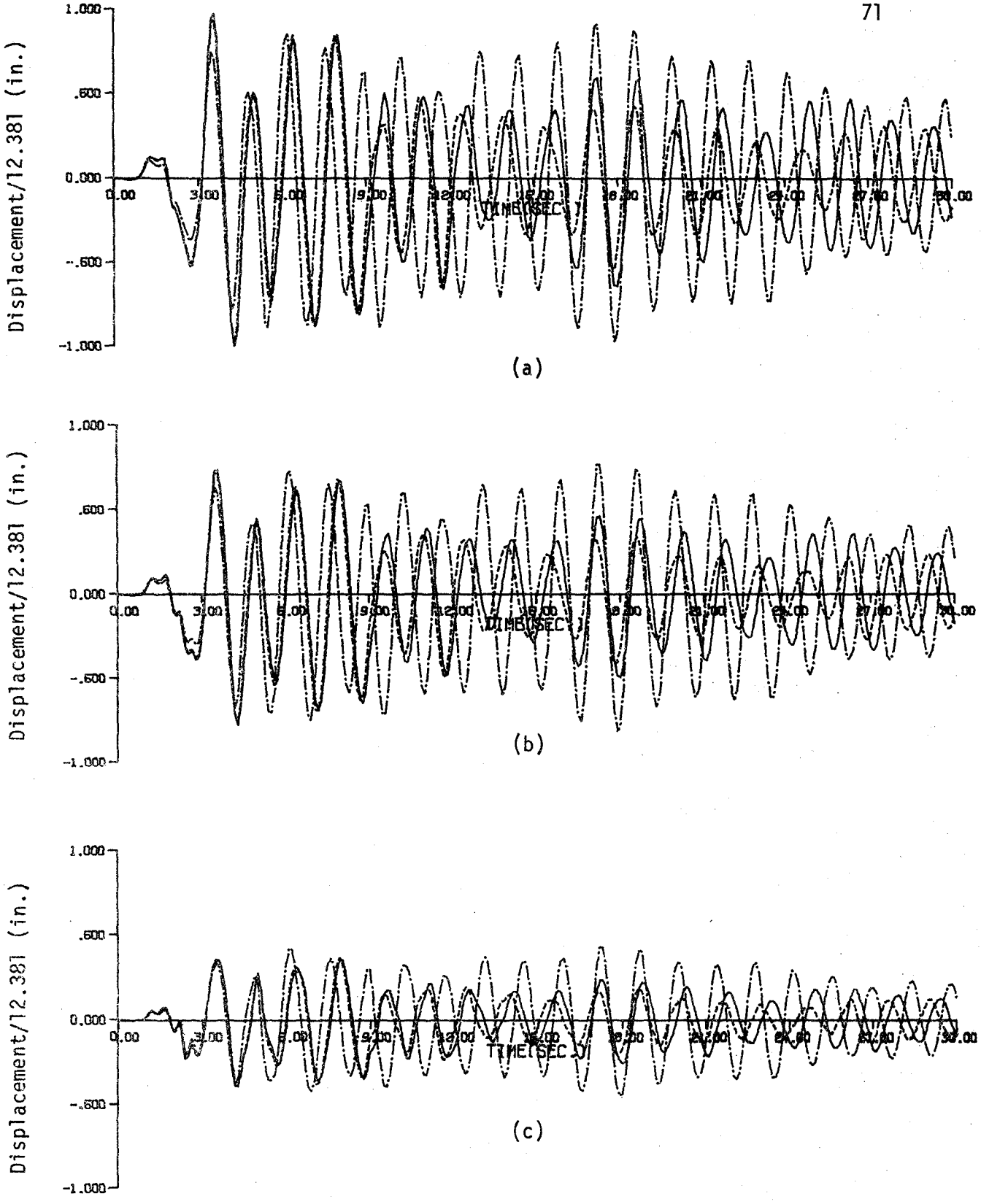

Figure 27 Time history responses (—— exact, —·—·—· shear beam, ---- Timoshenko beam): (a) the 15th story; (b) the 10th story; (c) the 5th story

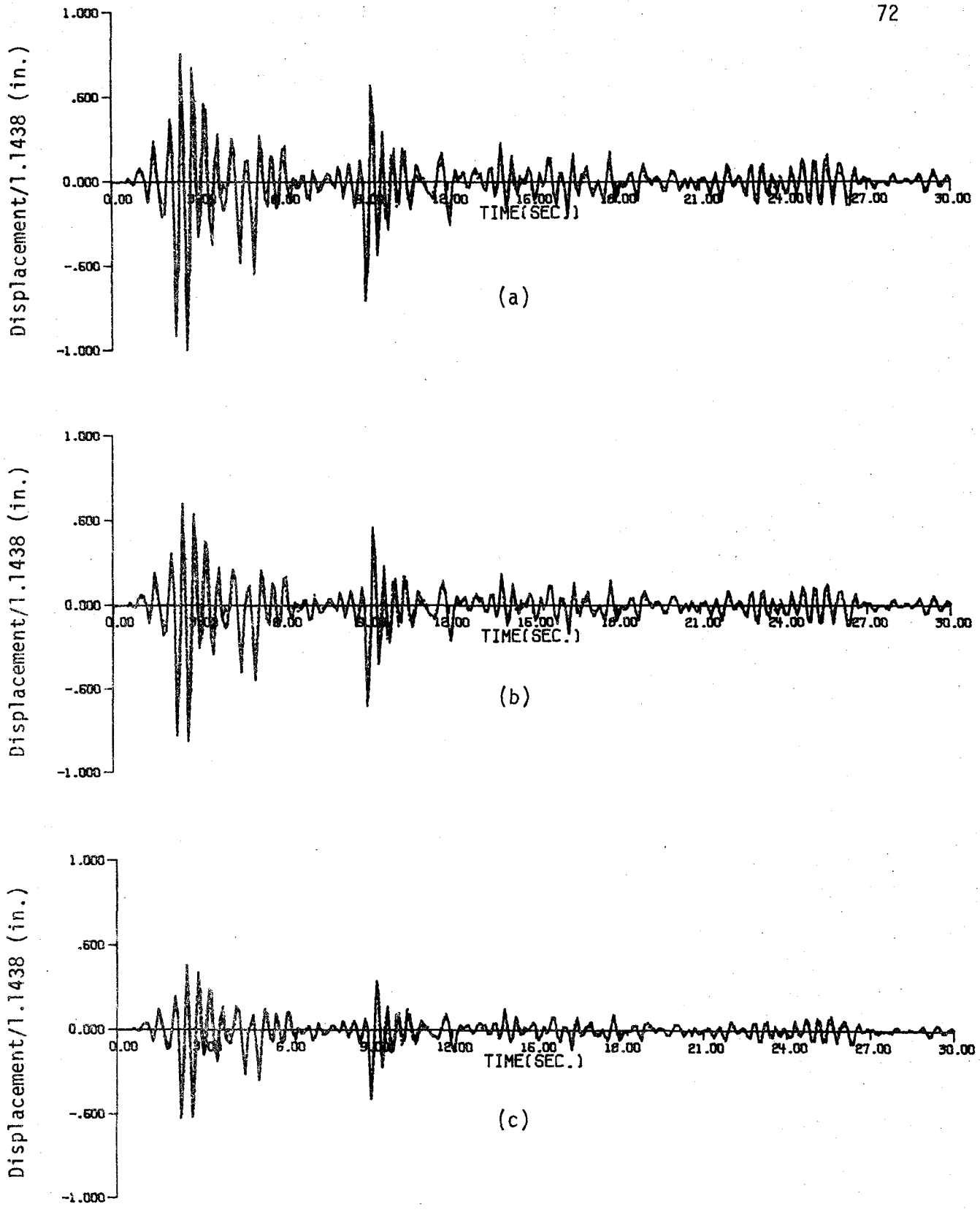

Figure 28 Time history responses (—— exact, —·—·—· shear beam, ---- Timoshenko beam): (a) the 7th story; (b) the 5th story; (c) the 3rd story

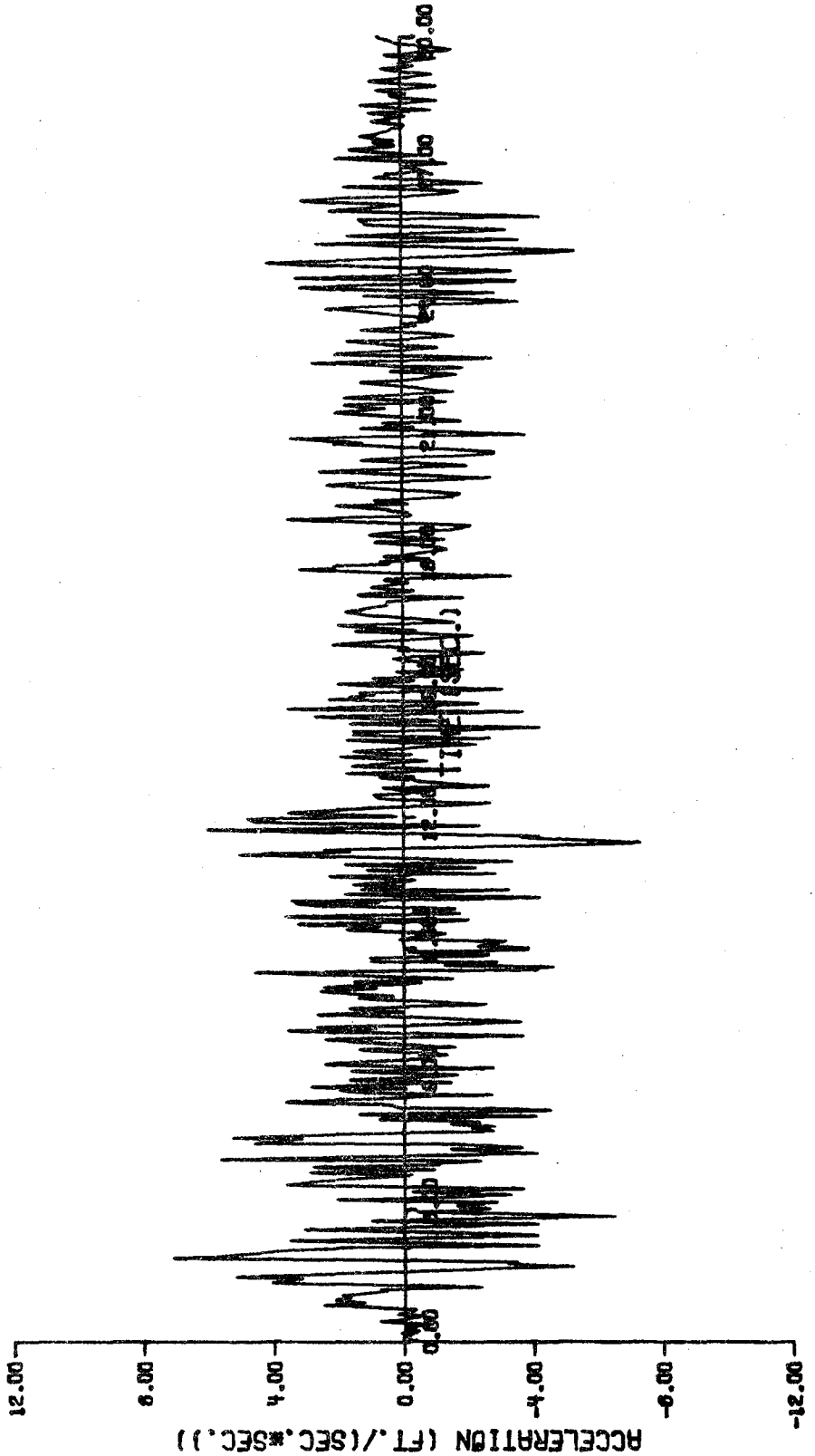

Figure 29 Accelerogram of E-W component for 30-second duration from El Centro Earthquake, May 18, 1940

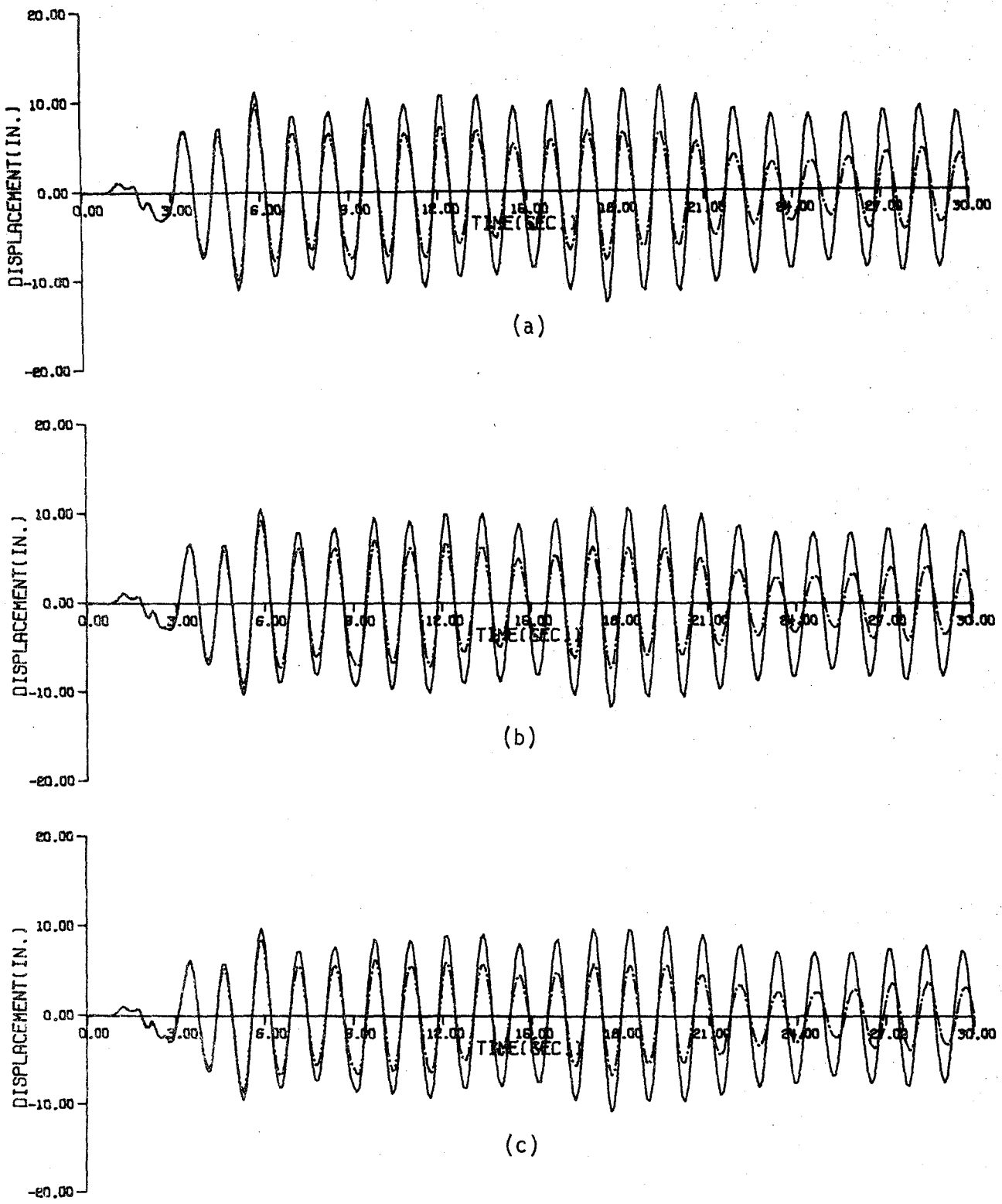

Figure 30 Simple shear beam model seismic responses for the total system of the power plant in N-S direction (—— zero damping, —·—·— with 1.5% critical damping): (a) at 245.0'; (b) at 191.0'; (c) at 169.0'

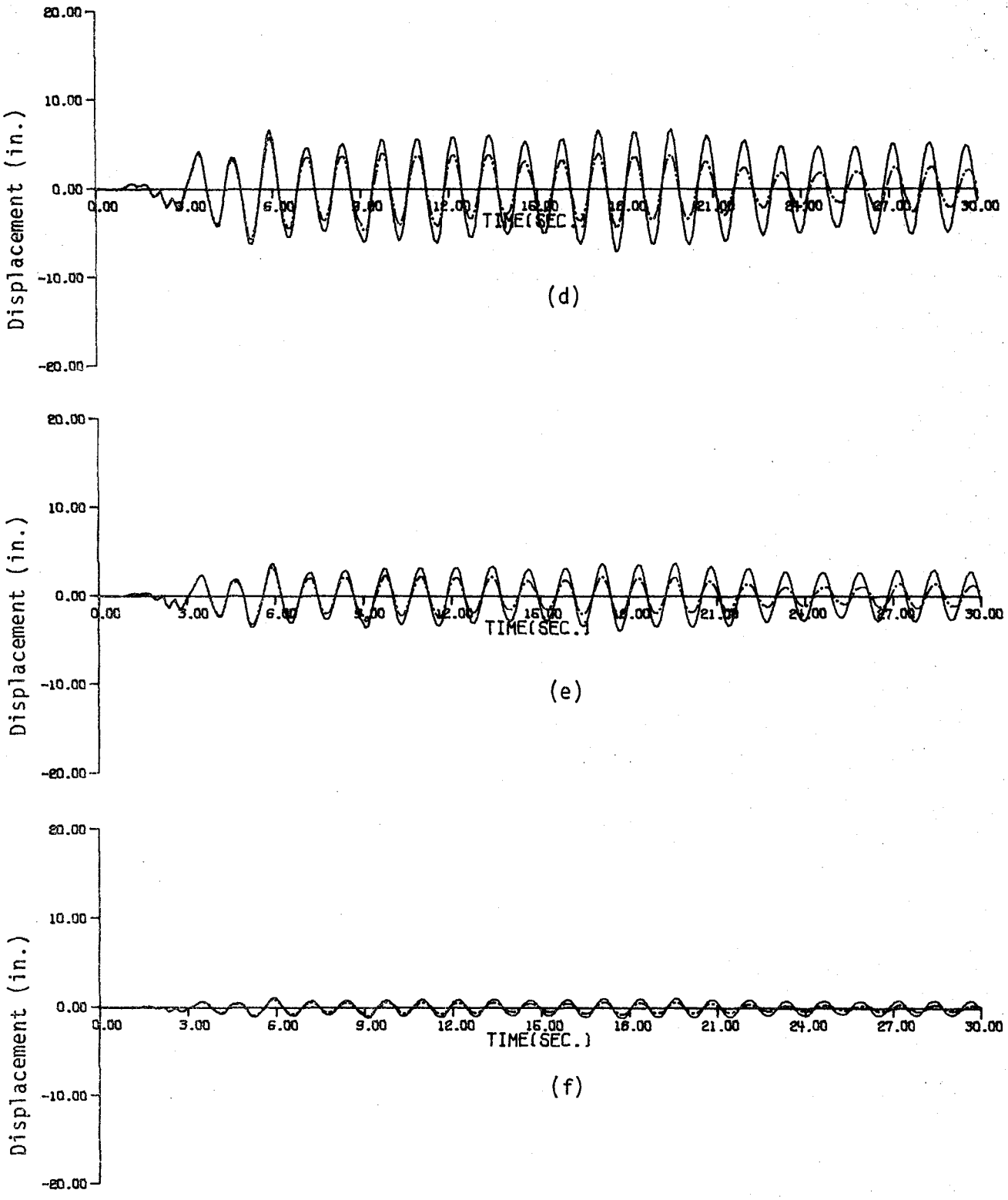

Figure 30 cont. (d) at 117.0'; (e) at 51.0'; (f) at 20.0'

the 1940 El Centro N-S and E-W acceleration components shown in Fig. 24 and Fig. 29 are performed. The N-S and E-W history responses at some story levels with zero damping are plotted as solid lines while those with 1.5% critical damping are traced with dash-dot lines as shown in Fig. 30 and Fig. 31, respectively. The maximum N-S displacement with zero damping is observed at t = 17.7 second with magnitude of 12.552 in. while an amplitude of 10.007 in. at t = 5.3 second is noted for the displacement with 1.5% critical damping. Those maximum displacements in E-W direction are 18.737 in. at t = 27.9 second with zero damping and 11.431 in. at t = 19.5 second with 1.5% critical damping as shown in Fig. 31. No exact history responses are available for comparison at this moment.

13. Dynamic Internal Force and Moment Computations using Simple Models

In design for earthquake resistance, the maximum stresses in the structure during the entire period of earthquake motion have to be computed. Since the simple models represent the gross behavior of a structure, the member stresses in the actual structure can not be obtained directly from the result of the simple model analysis. In this section, procedures are developed for recovering the member stresses from the simple models.

We assume that the displacement of the actual structure at each floor level is the same as that obtained from the simple models at any time of interest. Since during an earthquake, columns are subjected to the most severe loads and failures of columns have been observed in damaged buildings, we will focus our attention on the evaluation of the dynamic internal forces, moments, and stresses in columns in this study.

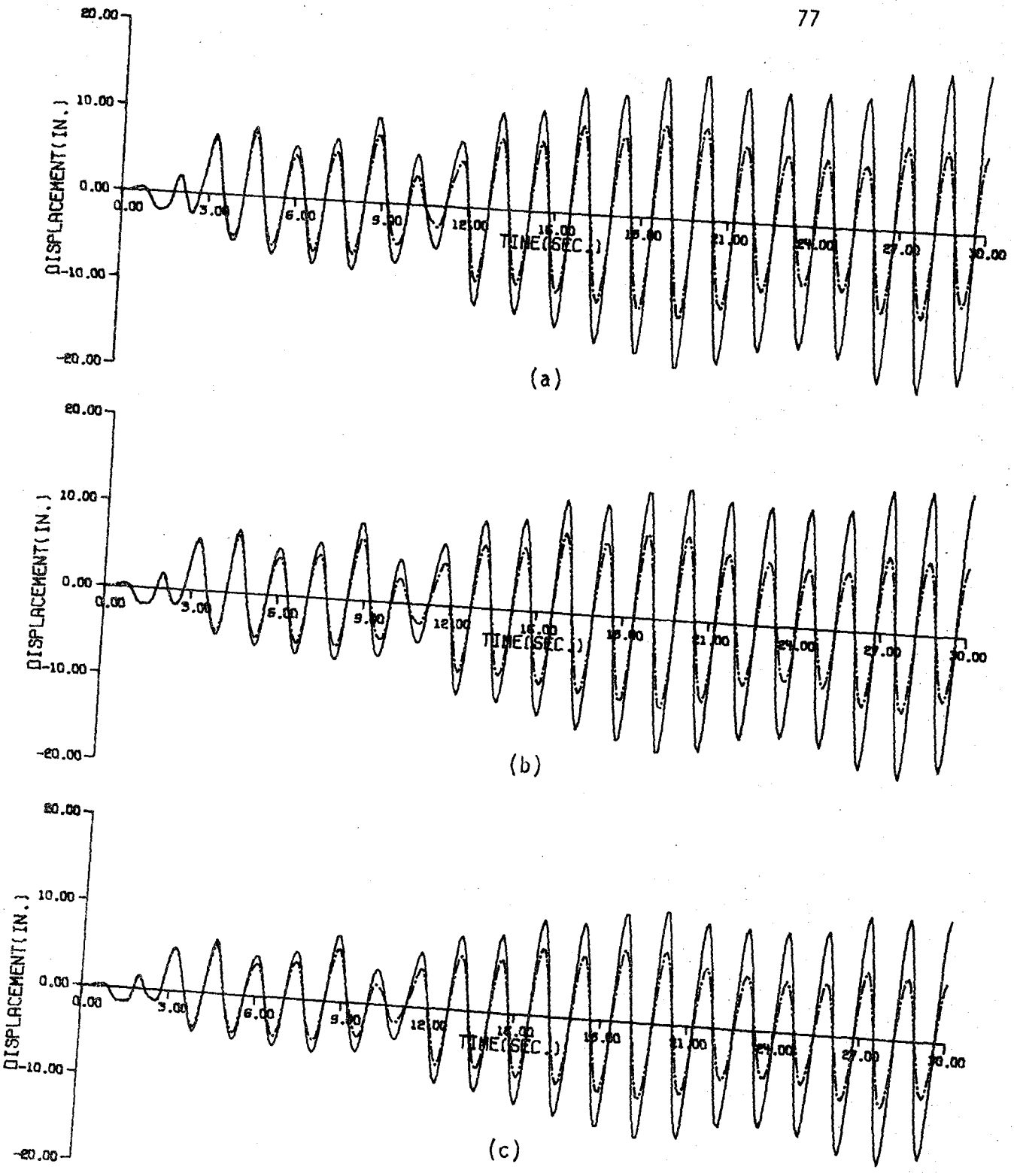

Figure 31 Simple shear beam model seismic responses for the total system of the power plant in E-W direction (—— zero damping, —·—·—· with 1.5% critical damping): (a) at 245.0'; (b) at 191.0'; (c) at 169.0'

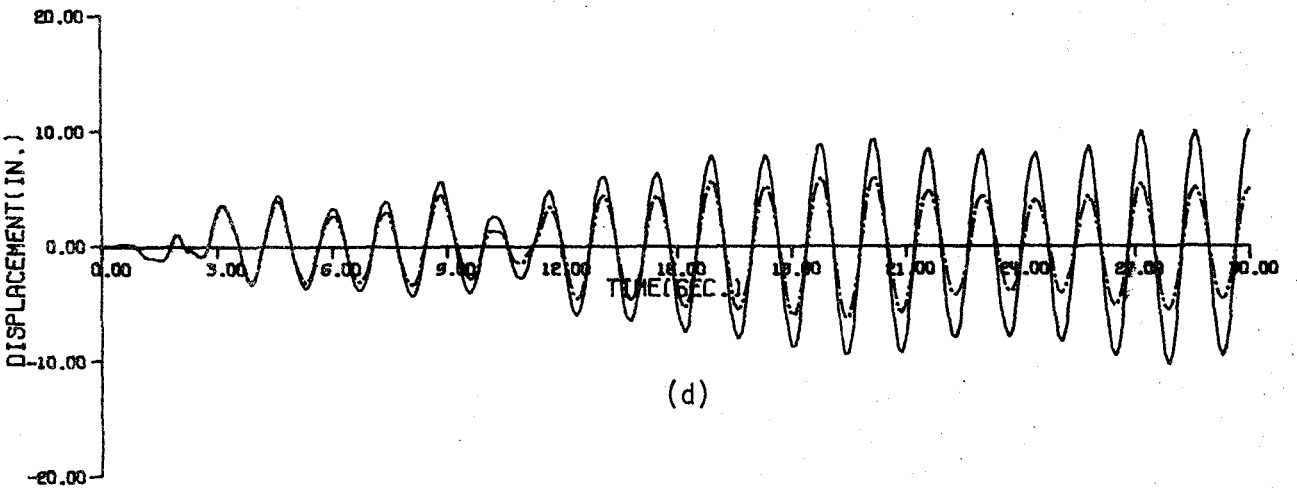

(d)

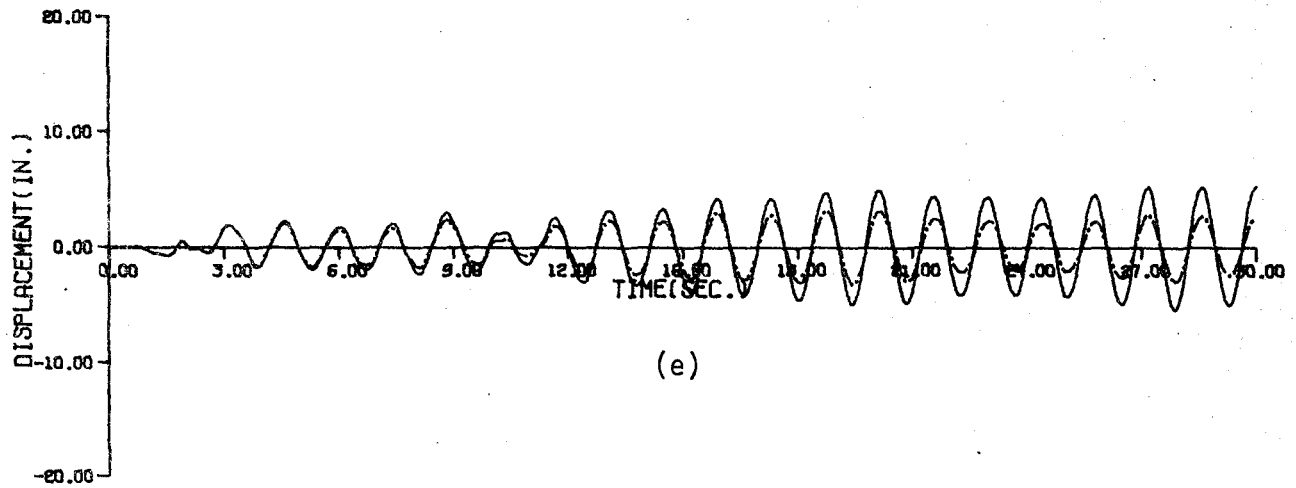

(e)

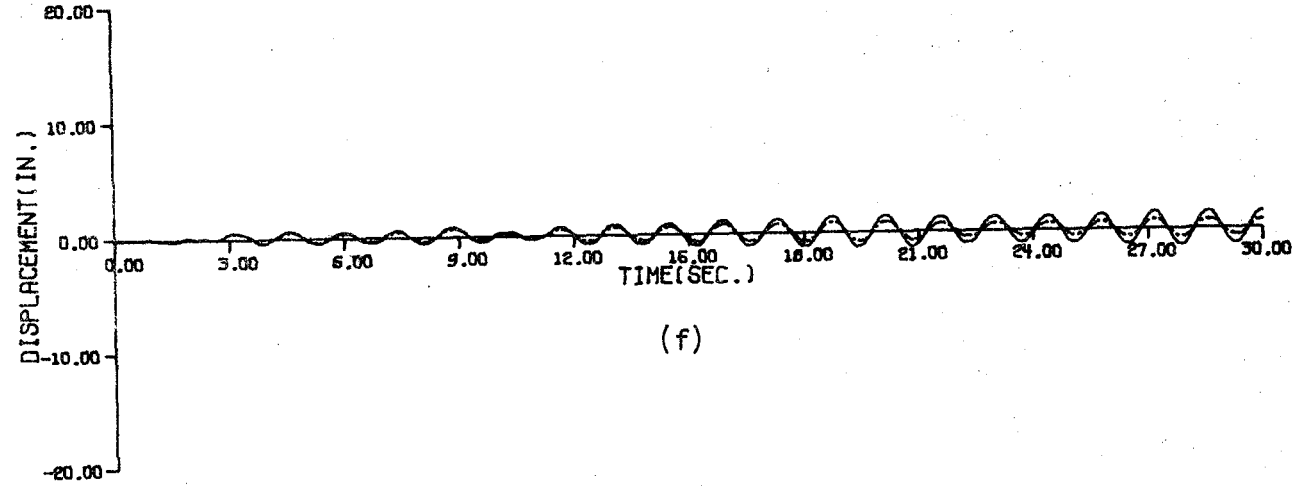

(f)

Figure 31 cont. (d) at 117.0'; (e) at 51.0'; (f) at 20.0'

At any time t, the displacements of the actual structure at the floor levels are taken to be the same values as given by the simple models. With this, the deformations in the substructures which were used to develop the simple models can be determined, and the forces and moments in the substructures can be easily computed. In the following, the procedures will be demonstrated for each substructure.

Consider first substructure Type a as shown in Fig. 2. The shear force V and bending moment M at the fixed end of the column can easily be obtained using the equilibrium condition of the member. We obtain

$$V = P$$

and

$$M = - P \frac{L_c}{2} \tag{70}$$

From Eqs. (1), (5) and (70) we have

$$V = 2(GA)_a \frac{\delta}{L_c}$$

and (71)

$$M = - (GA)_a \delta$$

Since δ is half of the true relative transverse displacement x between two adjacent floors, the shear force V and bending moment M at the fixed end of the solumn should be

$$V = (GA)_a \frac{x}{L_c}$$

and (72)

$$M = - \frac{1}{2} (GA)_a x$$

In the same manner, the shear forces and bending moments of the columns other than Type a are

$$V = (GA)_b \frac{x}{L_c}$$

and (73)

$$M = -\frac{1}{2}(GA)_b x$$

for substructure Type b,

$$V = (GA)_c \frac{x}{L_c}$$

$$M_I = -\frac{2+3\alpha\beta}{2(1+3\alpha\beta)}(GA)_c x \quad (74)$$

and

$$M_J = -\frac{3\alpha\beta}{2(1+3\alpha\beta)}(GA)_c x$$

for substructure Type c, and

$$V = (GA)_d \frac{x}{L_c}$$

$$M_I = -\frac{1+3\alpha\beta}{1+6\alpha\beta}(GA)_d x \quad (75)$$

and

$$M_J = -\frac{3\alpha\beta}{1+6\alpha\beta}(GA)_d x$$

for substructure Type d. In Eqs. (72-75), x is the relative transverse displacement between the two adjacent floors and the subscripts I and J in Eqs. (74-75) are referred to the bottom and upper ends of the column. The parameters α and β in the last two equations are defined in Eq. (2).

With these formulas in hand, the dynamic internal forces, moments, and stresses in each column can be obtained. Since only the maximum values during the whole period of excitation are of interest, an attempt is made to seek these values without combing through the whole response history for each member.

To illustrate this procedure, the 4-Bay, 7-Story frame structure considered in Sec. 12 is chosen. The deformed shapes of the Timoshenko

beam at t = 4.8 second and t = 9.9 second are noted to bear close resemblance to the first natural mode shape. These deformed shapes as well as the first natural mode shape are normalized and presented in Table 11. In view of the foregoing, it is reasonable to assume that each column has its maximum internal shear forces and bending moments at a particularly certain time t when the maximum displacement occurs. Following this procedure, the internal shear forces and bending moments for each column are obtained by using the Timoshenko beam model. The results together with those using the "exact" finite element method at t = 4.8 sec. and at t = 9.9 sec. are given in Table 12 and Table 13, respectively. At these two instants, the displacements appear to assume maximum values. It is noted that, in this history response analysis, ten modes are taken for mode superposition in the exact response solutions while only two modes are used in the Timoshenko model solutions. Due to the existence of symmetry, only half of the results are shown in the table. It is found that the columns located between the base and the first story have the maximum shear forces as well as bending moments for both cases. Among these columns, the one between the first bay and the second bay is found to be most critical.

14. Conclusions

A simple shear beam model and a Timoshenko beam model for vibration analysis of frame structures are presented. Explicit formulas for evaluating the effective stiffnesses are derived. Modified effective shear rigidity for the situation that local bending effect occurs is also presented. Finite elements based upon these simple models are also formulated. The simple models are applied to predict the first two

Story No.	Transverse Displacement at T = 4.8 sec.	Transverse Displacement at T = 9.9 sec.	First Mode Shape
1	0.1523	0.1475	0.1483
2	0.3644	0.3543	0.3561
3	0.5618	0.5497	0.5517
4	0.7311	0.7205	0.7222
5	0.8636	0.8569	0.8580
6	0.9540	0.9516	0.9519
7	1.0	1.0	1.0

Table 11 Normalized transverse displacement vs. Normalized first mode shape

Column-Story No.	Shear Forces x 10^{-2} (LB)		Bending moments x 10^{-5} (LB-IN)			
	Exact	Timoshenko Beam	Exact		Timoshenko Beam	
			M(I)	M(J)	M(I)	M(J)
1-1	-95.080	-93.845	18.251	10.273	17.596	10.558
1-2	-64.824	-76.233	9.533	9.914	11.435	11.435
1-3	-57.063	-70.968	8.238	8.881	10.645	10.645
1-4	-48.645	-60.844	6.832	7.761	9.127	9.127
1-5	-37.973	-47.637	5.063	6.330	7.146	7.146
1-6	-24.662	-32.494	2.893	4.506	4.874	4.874
1-7	-6.419	-16.541	0.383	1.543	2.481	2.481

Table 12 Dynamic internal shear forces and bending moments at T = 4.8 second

Column-Story No.	Shear Forces x 10^{-2} (LB)		Bending moments x 10^{-5} (LB-IN)			
	Exact	Timoshenko Beam	Exact		Timoshenko Beam	
			M(I)	M(J)	M(I)	M(J)
2-1	-122.72	-114.96	21.030	15.788	19.707	14.781
2-2	-114.27	-114.35	17.197	17.083	17.152	17.152
2-3	-100.24	-106.45	14.797	15.275	15.968	15.968
2-4	-87.16	-91.27	12.759	13.390	13.690	13.690
2-5	-69.64	-71.46	10.006	10.887	10.718	10.718
2-6	-47.01	-48.74	6.521	7.583	7.311	7.311
2-7	-21.82	-24.81	2.756	3.788	3.722	3.722

Table 12 cont.

Column-Story No.	Shear Forces x 10^{-2} (LB)		Bending moments x 10^{-5} (LB-IN)			
	Exact	Timoshenko Beam	Exact		Timoshenko Beam	
			M(I)	M(J)	M(I)	M(J)
3-1	-120.84	-114.96	20.846	15.406	19.707	14.781
3-2	-112.49	-114.35	16.817	16.931	17.152	17.152
3-3	-101.47	-106.45	14.949	15.492	15.968	15.968
3-4	-89.75	-91.27	13.111	13.813	13.690	13.690
3-5	-73.48	-71.46	10.555	11.490	10.718	10.718
3-6	-51.84	-48.74	7.224	8.327	7.311	7.311
3-7	-29.03	-24.81	3.733	4.974	3.722	3.722

Table 12 cont.

Column-Story No.	Shear Forces x 10^{-2} (LB)		Bending moments x 10^{-5} (LB-IN)			
	Exact	Timoshenko Beam	Exact		Timoshenko Beam	
			M(I)	M(J)	M(I)	M(J)
1-1	-88.605	-98.898	17.463	9.119	18.543	11.126
1-2	-75.120	-80.914	11.526	11.010	12.137	12.137
1-3	-69.762	-76.433	10.172	10.756	11.465	11.465
1-4	-58.013	-66.810	8.066	9.338	10.022	10.022
1-5	-43.051	-53.375	5.632	7.284	8.006	8.006
1-6	-26.570	-37.006	3.040	4.931	5.551	5.551
1-7	-6.338	-18.950	0.316	1.585	2.843	2.843

Table 13 Dynamic internal shear forces and bending moments at T = 9.9 second

Column-Story No.	Shear Forces x 10^{-2} (LB)		Bending moments x 10^{-5} (LB-IN)			
	Exact	Timoshenko Beam	Exact		Timoshenko Beam	
			M(I)	M(J)	M(I)	M(J)
2-1	-117.06	-121.15	20.323	14.797	20.768	15.576
2-2	-129.55	-121.37	19.773	19.093	18.206	18.206
2-3	-121.10	-114.65	17.959	18.370	17.197	17.197
2-4	-103.46	-100.22	15.091	15.948	15.032	15.032
2-5	-79.27	-80.06	11.319	12.462	12.009	12.009
2-6	-51.36	-55.51	7.079	8.330	8.326	8.326
2-7	-23.18	-28.43	2.910	4.043	4.264	4.264

Table 13 cont.

Column-Story No.	Shear Forces x 10^{-2} (LB)		Bending moments x 10^{-5} (LB-IN)			
	Exact	Timoshenko Beam	Exact		Timoshenko Beam	
			M(I)	M(J)	M(I)	M(J)
3-1	-115.32	-121.15	20.153	14.444	20.768	15.576
3-2	-127.79	-121.37	19.410	18.929	18.206	18.206
3-3	-122.21	-114.65	18.085	18.578	17.197	17.197
3-4	-106.28	-100.22	15.469	16.415	15.032	15.032
3-5	-83.65	-80.06	11.942	13.154	12.009	12.009
3-6	-56.93	-55.51	7.890	9.187	8.326	8.326
3-7	-31.44	-28.43	4.031	5.402	4.264	4.264

Table 13 cont.

flexural modes in the principal planes of the fossil fuel power plant of Unit #3 of TVA at Paradise, Kentucky. Comparisons of the simple model solutions with the exact finite element solutions show that the present simple models are quite adequate in predicting the natural frequencies and the corresponding mode shapes for the lower modes. When the frame structures are heavily braced, it is found that longitudinal motion might appear in the lower modes of vibration. A model of axial member for the longitudinal motion is also derived.

The simple models proposed in this report could be very useful in seismic dynamic analysis of engineering frame structures where lower modes usually dominate the response. The models are extended to predict with great accuracy the time history responses of the dynamic internal column shear forces and bending moments caused by earthquakes.

References:

1. Goldberg, J. F., Bogdanoff, J. L., and Moh, Z. L., "Forced Vibration and Natural Frequencies of Tall Building Frames," Bulletin of the Seismological Society of America 49, 1959, pp. 33-47.

2. Paramasivam, P., Yeh, C. S., and Nassim, S., "Dynamic Analysis of Building Frames," Journal of Sound and Vibration, 1975, pp. 103-112.

3. Sandhu, B. S., "Dynamic Analysis of Multistory Buildings," Engineering Journal/AISC, 1974, pp. 67-72.

4. Heidebrecht, A. C., and Smith, B. S., "Approximate analysis of Tall Wall-Frame Structures," Journal of Structural Division, ASCE, Vol. 99, ST2, 1973, pp. 199-221.

5. Blume, J. A., "Structural Dynamics of Cantilever Type Buildings," Proceedings of Fourth World Conference on Earthquake Engineering, Vol. 2, Chile, 1969, pp. A3 1-18.

6. Blume, J. A., "Dynamic Characteristics of Multistory Buildings," Journal of Structural Division, ASCE, Vol. 94, ST2, 1968, pp. 377-402.

7. Clough, R. W. and Jenschke, V. A., "The Effect of Diagonal Bracing on the Earthquake Performance of a Steel Frame Building," Bulletin of the Seismological Society of America, Vol. 53, No. 2, 1963, pp. 389-401.

8. Fung, Y. C., Foundations of Solid Mechanics, Prentice-Hall, 1965.

9. Bathe, K. J., Wilson, E. L., and Peterson, F. E., "SAP IV - A Structural Analysis Program for Static and Dynamic Response of Linear System," Earthquake Engineering Research Center, University of California, Berkley, California, EERC 73-11, June, 1973, Revised April, 1974.

10. Yang, T. Y., Baig, M. I., and Bogdanoff, J. L., "Seismic Structural Response of Steam Generators and Their Supporting Structures," Technical report submitted to the National Science Foundation, April 1978.

11. Bathe, K. J. and Wilson, E. L., Numerical Methods in Finite Element Analysis, Prentice-Hall, Inc., Englewood Cliffs, N. J., 1976.

12. Meirovitch, L., Analytical Methods in Vibrations, the MacMillan Company, Collier-MacMillan Limited, London, 1967.

13. Clough, R. W. and Penzien, J., Dynamics of Structures, McGraw-Hill, Inc., 1975.

14. Clough, R. W., "On the Importance of Higher Modes of vibration in Earthquake Response of Tall Buildings," Bulletin of the Seismological Society of America, Vol. 45, No. 4, 1955, pp. 289-301.

15. Wilson, E. L. and Penzien, J., "Evaluation of Orthogonal Damping Matrices," International Journal for Numerical Methods in Engineering, Vol. 4, 1972, pp. 5-10.

16. Bathe, K. J. and Wilson, E. L., "Stability and Accuracy Analysis of Direct Integration Methods," Earthquake Engineering and Structural Dynamics, Vol. 1, 1973, pp. 283-291.

17. Humar, J. L. and Wright, E. W., "Earthquake Response of Steel-Frame Multistory Buildings with Set-Backs," Earthquake Engineering and Structural Dynamics, Vol. 5, 1977, pp. 15-39.